

SWx impacts on ionospheric wave propagation - *focus on GNSS and HF*



Collaboration of



Solar-Terrestrial Centre of Excellence

UNIVERSITY OF TWENTE | RADIO SYSTEMS



Koninklijk Nederlands
Meteorologisch Instituut
Ministerie van Infrastructuur en Milieu



EXTREME EVENTS and IMPACTS

Jan Janssens

Solar-Terrestrial Centre of
Excellence (STCE)

Belgium



Image credits: ESA / J. Huart

https://www.esa.int/ESA_Multimedia/Images/2000/09/Galileo_satellite_system

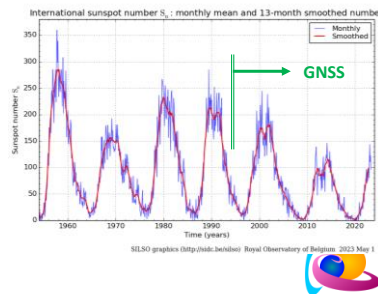
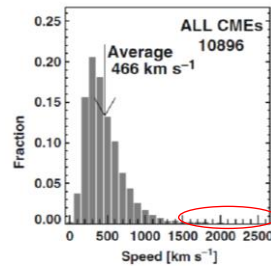
Contents

- What is an extreme event?
- SWx drivers & impacts: overview
- **GNSS** impacts from
 - Solar flares & solar radio bursts
 - Solar energetic particle events
 - Interplanetary coronal mass ejections
 - High speed streams from coronal holes



What is an extreme event?

- No very concrete definition:
 - Tail's end of a distribution
 - No one-on-one correlation between frequency and impact
 - E.g. July 2012 farside event
 - Boundary conditions
 - Day/night,...
 - Low probability, high impact event
 - Only 20-30 years of GNSS data
 - 1 moderate and 1 weak solar cycle since the mid-1990s...



4

Annotated figures credits:

Gopalswamy, 2010: Corona Mass Ejections: a Summary of Recent Results
<https://ui.adsabs.harvard.edu/abs/2010nspm.conf..108G/abstract>

The definition of an extreme event is not very concrete, but can be thought of as an event on the tail of a distribution. An extreme event can also be thought of as an occurrence that has unique characteristics in its origin and/or in its consequences. ... We are interested in extreme events both in their origins at the Sun and their consequences and space weather effects.

SILSO: <https://www.sidc.be/SILSO/home>

Data for GNSS and GNSS impacts is limited:

GPS: Globally available since 1994 ; 32 satellites

GLONASS: Full global coverage since 1995 ; 24 satellites

Beidou: operational since 2012 ; 35 satellites

Galileo: operational since 2016 ; 24 satellites

24 satellites is a minimum for global GNSS coverage

What is an extreme event?

Solar Cycle	SC21	SC22	SC23	SC24	SC25
Period	1976-1986	1986-1996	1996-2008	2008-2019	2019-present
Highest monthly sunspot number (ISN)	266.9 Sep 1979	284.5 Jun 1989	244.3 Jul 2000	146.1 Feb 2014	160.5 Jun 2023
Highest monthly sunspot area (in MH)	3719.0 Feb 1982	3666.6 Jun 1989	3000.2 Sep 2001	2015.2 Feb 2014	1870.6 Jul 2023
Highest monthly 10.7 cm radio flux (1AU; in sfu)	229.1 May 1980	247.2 Jun 1989	236.2 Sep 2001	166.0 Feb 2014	183.3 Jul 2023
Strongest flare*	X21 NOAA 1203 11 Jul 1978	X28 NOAA 5629 16 Aug 1989	X40 NOAA 10486 4 Nov 2003	X13 NOAA 12673 6 Sep 2017	X2.2 NOAA 12992 20 Apr 2022
Total number of X-class flares*	261	233	182	76	20
Strongest proton event (> 10 MeV; in pfu)	2900 13 Jul 1982	43000 24 Mar 1991	31700 6 Nov 2001	6530 8 Mar 2012	620 18 Jul 2023
Number of proton events (> 10 MeV)	59	73	94	42	18
Number of Ground Level Enhancements (GLE)	13	15	16	2	1 28 Oct 2021
Number of days with Kp ≥ 8-	42	42	43	9	4
Strongest Dst (in nT)	-325 14 Jul 1982	-589 13-14 Mar 1989	-422 20 Nov 2003	-234 17 Mar 2015	-212 24 Apr 2023

* : The GOES-1 thru -15 flare data have been corrected for the scaling factors.



Data updated until 29 November 2023. Data sources:

- SILSO: WDC for the International Sunspot Number Brussels: <https://www.sidc.be/SILSO/home>
- Solar Cycle Science: <http://solarcyclescience.com/index.html>
- WDC for geomagnetism Kyoto: <https://wdc.kugi.kyoto-u.ac.jp/index.html>
- GeoForschungsZentrum (GFZ) Potsdam: <https://kp.gfz-potsdam.de/en/data>
- University of Oulu: <https://gle oulu.fi/#/>
- NOAA/SWPC: <ftp://ftp.swpc.noaa.gov/pub/indices/SPE.txt>
- Penticton, Canada: <https://www.spaceweather.gc.ca/forecast- prevision/solar-solaire/solarflux/sx-5-mavg-en.php>
- NOAA/NGDC: <ftp://ftp.ngdc.noaa.gov/STP/space-weather/solar-data/solar-features/solar-flares/x-rays/goes/>
- NOAA/SWPC Weekly bulletins: <ftp://ftp.swpc.noaa.gov/pub/warehouse/>
- Note the flare values from GOES-1 thru -15 (SC21 thru ~SC24) have been corrected i.a.w. guidelines by NGDC/NOAA at <https://www.ngdc.noaa.gov/stp/satellite/goes/index.html>
- For SC25, there are so far 2 ARs which produced the strongest flare (X2.2): NOAA12992 on 20 April 2022, and NOAA 13229 on 17 February 2023.

Acronyms: **SC:** Solar Cycle ; **ISN:** International Sunspot Number ; **MH:** Millionths of a solar hemisphere ; **AU:** Astronomical Unit ; **sfu:** solar flux units ; **MeV:** Mega electronvolt ; **pfu:** particle flux units ; **Kp:** planetary K-index ; **Dst:** Disturbance storm time index ; **nT:** nano Tesla

What is an extreme event?

Observed, statistically expected, and modelled extreme solar and solar-terrestrial events (based on Cliver et al. 2022 ; Gopalswamy 2018)

Parameter	Observed Extremum	100-year ev. Exp. Law	100-year ev. Power Law	1000-year ev. Exp. Law	1000-year ev. Power Law	Modelled Extremum
Sunspot group area (MH)	6132	5800	7100	8200	13600	
GOES flare SXR	X40	X44	X42	X100	X115	X180
1.5 GHz radio emission (10^9 sfu)	1		3.2 - 12		61 - 200	
> 30 MeV proton fluence (10^{10} cm ⁻²)	0.84	1.6	2.1	5	16	
> 200 MeV proton fluence (10^{10} cm ⁻²)	0.14	0.6		3.5		
CME speed (km/s)	3387	3800	4500	4700	6600	
ICME transit time (h)	14.6					11.6
Dst (nT)	-950	-603	-774	-845	-1470	-2000 to -2500

Acronyms: **ev.:** event ; **Exp. Law:** exponential law ; **MH:** Millionths of a solar hemisphere ; **GOES:** Geostationary Operational Environmental Satellite ; **SXR:** soft x-rays ; **GHz:** gigahertz ; **sfu:** solar flux units ; **MeV:** Mega electronvolt ; **pfu:** particle flux units ; **(I)CME:** (Interplanetary) Coronal Mass Ejection ; **Kp:** planetary K-index ; **Dst:** Disturbance storm time index ; **nT:** nano Tesla

Summary based on

Cliver et al. 2022: Extreme solar events - <https://doi.org/10.1007/s41116-022-00033-8> (Table 10) and

Gopalswamy 2018: Extreme solar eruptions and their space weather consequences - <https://doi.org/10.1016/B978-0-12-812700-1.00002-9> (Table 2)

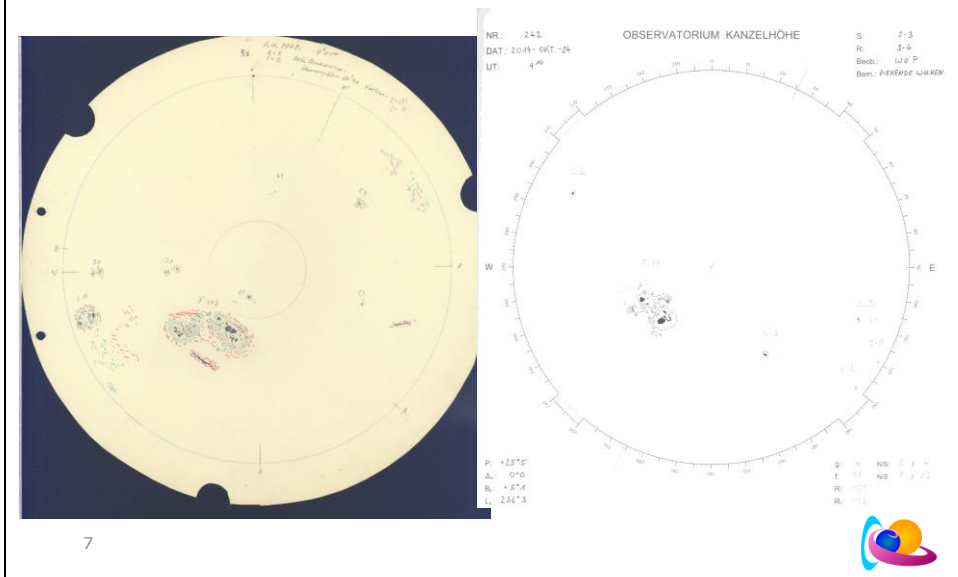
Events related to the observed extrema (Column 2): Sunspot area: 8 April 1947 (Greenwich #1488603) ; GOES flare SXR (corrected*): 4 November 2003 (NOAA 10486) ; 1.5 GHz radio emission: 6 December 2006 (NOAA 10930) ; >30 MeV fluence: August 1972 event ; >200 MeV fluence: 23 February 1956 ; CME speed: 10 November 2004 (NOAA 10696) ; ICME transit: 4 August 1972 (Greenwich #2317900) ; Dst: based on the 2 September 1859, 4 February 1872 and 15 May 1921 geomagnetic storms which all 3 had minimum Dst values around -950 nT.

Power law distributions in general appear to yield overestimates.

* Note the flare values from GOES-1 thru -15 (SC21 thru ~SC24) have been corrected i.a.w. guidelines by NGDC/NOAA at <https://www.ngdc.noaa.gov/stp/satellite/goes/index.html> The X28 flare of 4 November 2003 thus turns out to be X40 . The Cliver et al. (2022) statistics also take these corrections into account.

Acronyms: **ev.:** event ; **Exp. Law:** exponential law ; **MH:** Millionths of a solar hemisphere ; **GOES:** Geostationary Operational Environmental Satellite ; **SXR:** soft x-rays ; **GHz:** gigahertz ; **sfu:** solar flux units ; **MeV:** Mega electronvolt ; **pr:** proton ; **pfu:** particle flux units ; **(I)CME:** (Interplanetary) Coronal Mass Ejection ; **Kp:** planetary K-index ; **Dst:** Disturbance storm time index ; **nT:** nano Tesla

Largest sunspot groups SC18 & 24



Largest sunspot groups on 8 April 1947 (Greenwich #1488603) and 24 Oct 2014 (NOAA 12192) with areas of resp. 6132 MH and 3850 MH. The latter value has been corrected for the Greenwich-to-NOAA transition (see the Solar Cycle Science webpage at <http://solarcyclescience.com/activerregions.html>).

Drivers of disturbed SWx

Solar eruptions

Solar corona

Magnetic Reconnection

Solar wind

Radiation

Particles

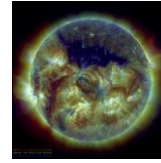
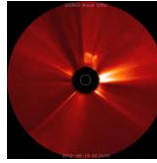
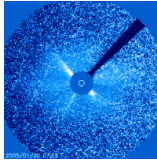
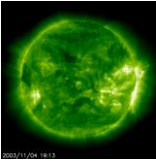
Particles

Solar flares

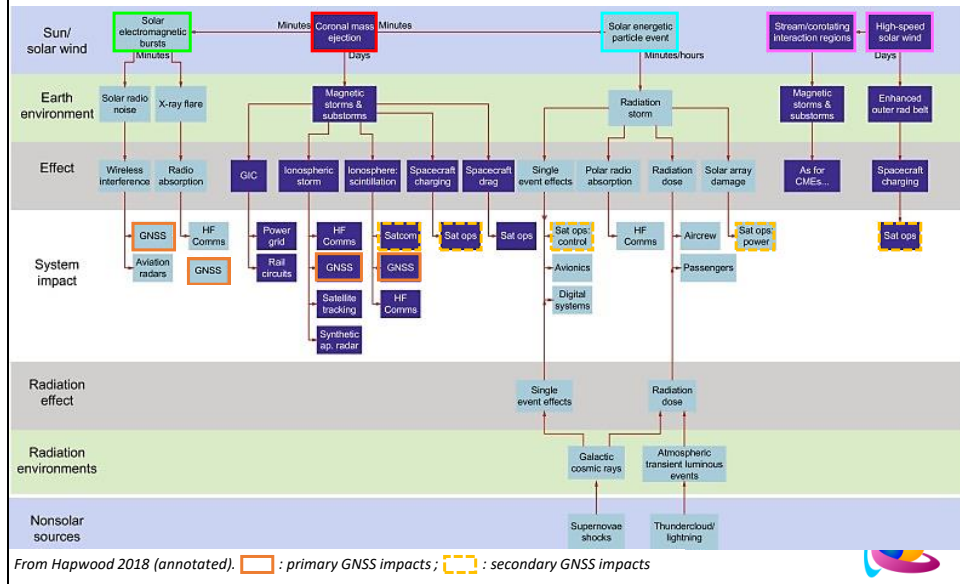
Proton events

Coronal Mass Ejections

Coronal Holes



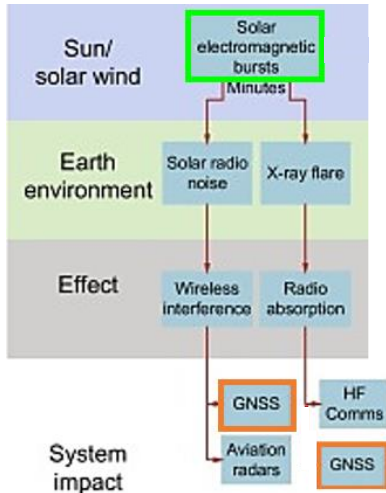
Impacts of disturbed SWx



Annotated from Hapgood, M. 2018. Linking Space Weather Science to Impacts - The View From the Earth
<https://doi.org/10.1016/B978-0-12-812700-1.00001-7> (Figure 1)

Important impacts on GNSS and GNSS applications are indicated in dark orange, less important are indicated in dashed light orange.

GNSS impacts from solar flares



- From EUV & X-ray

- Solar flare effect
 - "magnetic crochet"
 - Up to +/- 100 nT
- Shortwave fadeout
 - "Radio Blackout"
 - Impact on HF Com
- GNSS disturbances

- From radio emission

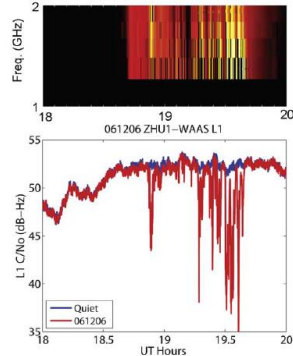
- GNSS disturbances
- Radar disturbances



Note there's also a non-solar source of highly energetic electromagnetic radiation that may affect the ionosphere (and VLF signals in particular): Gamma-Ray Bursts (GRB). See e.g. <https://www.stce.be/news/610/welcome.html>

GNSS impacts from solar flares

- From radio emission
 - 6 Dec 2006: X6.5
 - 1415 MHz: 10^6 sfu



11 Figure 2. Response of a GPS receiver to the solar radio burst on 6 December 2006. The red line corresponds to C/N_0 on 6 December 2006, and the blue line corresponds to the previous sidereal day.

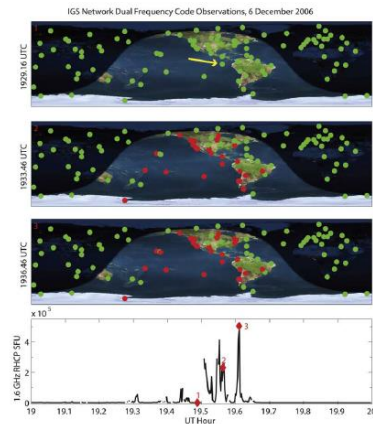


Figure 6. Receivers in the Global GPS Network that were analyzed during the solar radio burst. Green indicates the normal number of satellites being tracked. (fourth panel) During the burst (power at 1.6 GHz), several sunlit receivers tracked fewer than the four satellites needed for a full positioning solution (marked in red). (Image of Earth from The Living Earth, 1996 and is used here by permission of the publisher. Day/night overlay created using Earth Viewer by J. Walker.)

Credits: Cerruti et al. (2008)

Acronyms: **MHz**: megahertz ; **GHz**: gigahertz ; **sfu**: solar flux units ; **C/N_0** : Carrier-to-Noise ratio ; **L1** : GPS frequency (1575.42 MHz) ; **dB**: decibel ($=10 \log_{10} (\text{Power}/\text{Power}_{\text{base}})$) ; **IGS**: International GNSS service ; **WAAS**: Wide Area Augmentation Service

Figures and text taken from:

Cerruti et al. (2008): Effect of intense December 2006 solar radio bursts on GPS receivers

<https://ui.adsabs.harvard.edu/abs/2008SpWea...610D07C/abstract>

On 6 December 2006, an X6 flare generated a solar radio burst with measured powers of 1,000,000 SFU RHCP [Right Hand Circularly Polarized] at 1.4 GHz, and lesser levels of 650,000 and 500,000 SFU at 1.2 and 1.6 GHz, respectively.

This solar radio burst had significant effects on GPS receivers over the entire sunlit hemisphere of Earth.

Solar radio bursts during December 2006 were sufficiently intense to be measurable with GPS receivers. The strongest event occurred on 6 December 2006 and affected the operation of many GPS receivers. This event exceeded 1,000,000 solar flux unit (SFU) and was about 10 times larger than any previously reported event. Prior to the events of December 2006, the record solar burst near the GPS frequencies, according to reports collected by the National Oceanic and Atmospheric Administration (NOAA), was 165,000 SFU at 1415 MHz for a SRB in April 1973. Second place was 88,000 SFU at 1415 MHz in February 1979.

The strength of the event was especially surprising since the solar radio bursts occurred near solar minimum. The strongest periods of solar radio burst activity lasted a few minutes to a few tens of minutes and, in some cases, exhibited large intensity differences between L1 (1575.42 MHz) and L2 (1227.60 MHz). Civilian dual frequency GPS receivers were the most severely affected, and these events suggest that continuous, precise positioning services should account for solar radio bursts in their operational plans. This investigation raises the possibility of even more intense solar radio bursts during the next solar maximum that will significantly impact the operation of GPS receivers.

The receiver indicated by the yellow arrow is located on the Galapagos Islands. It was the receiver closest to the subsolar point at that time.

The 6 December event marks the first time a SRB was detected on the FAA (Federal Aviation Administration) WAAS.

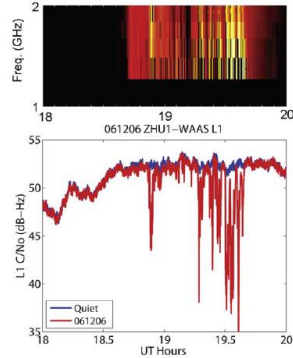
Although the effects of this SRB were less intense on WAAS than on other operational systems, mainly because of the robust system design, it is important to consider the potential impact of future, more powerful, solar radio bursts during periods of high solar activity.

... / ...

Acronyms: **MHz**: megahertz ; **GHz**: gigahertz ; **sfu**: solar flux units ; **C/N_0** : Carrier-to-Noise ratio ; **L1** : GPS frequency (1575.42 MHz) ; **dB**: decibel ($=10 \log_{10} (\text{Power}/\text{Power}_{\text{base}})$) ; **IGS**: International GNSS service ; **WAAS**: Wide Area Augmentation Service

GNSS impacts from solar flares

- From radio emission
 - 6 Dec 2006: X6.5
 - 1415 MHz: 10^6 sfu



12 Figure 2. Response of a GPS receiver to the solar radio burst on 6 December 2006. The red line corresponds to C/N_0 on 6 December 2006, and the blue line corresponds to the previous sidereal day.

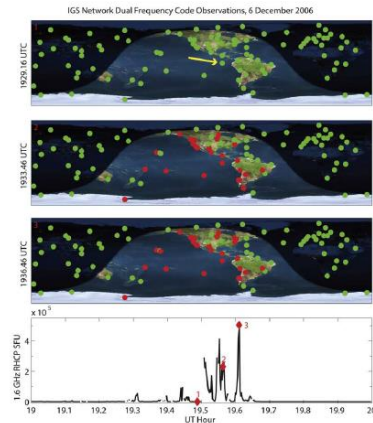


Figure 6. Receivers in the Global GPS Network that were analyzed during the solar radio burst. Green indicates the normal number of satellites being tracked. (fourth panel) During the burst (power at 1.6 GHz), several sunlit receivers tracked fewer than the four satellites needed for a full positioning solution (marked in red). (Image of Earth from The Living Earth, 1996 and is used here by permission of the publisher. Day/night overlay created using Earth Viewer by J. Walker.)

Credits: Cerruti et al. (2008)

Acronyms: MHz: megahertz ; GHz: gigahertz ; sfu: solar flux units ; C/N_0 : Carrier-to-Noise ratio ; L1 : GPS frequency (1575.42 MHz) ; dB: decibel ($=10 \log_{10} (\text{Power}/\text{Power}_{\text{base}})$) ; IGS: International GNSS service ; WAAS: Wide Area Augmentation Service

Figures and text taken from:

Cerruti et al. (2008): Effect of intense December 2006 solar radio bursts on GPS receivers

<https://ui.adsabs.harvard.edu/abs/2008SpWea...610D07C/abstract>

... / ...

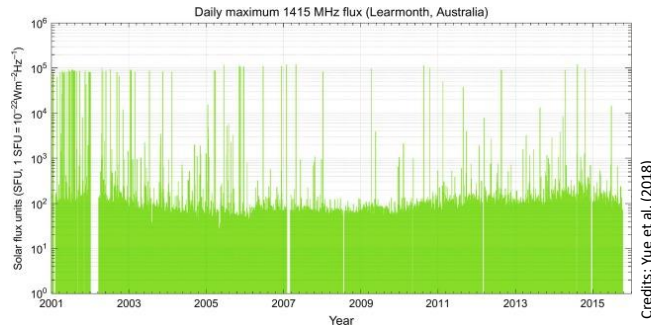
For the original scientific purpose of long-term geodetic monitoring, solar radio bursts have a negligible impact because they are short-lived (tens of minutes) compared to the timescales over which geodetic changes are being monitored. Data loss, even though worldwide, has minimal implications to geodetic science. However, these same receivers have been adapted for other uses, including a few critical real-time applications that rely on round-the-clock 24/7 availability of the GPS signals (an example is the positioning of offshore oil rigs discussed in section 3.3). These high-precision real-time positioning applications require that users receive dual frequency corrections to their GPS signals within a few seconds of real time. Global positioning accuracies of 10–20 cm have been demonstrated with such systems. The real-time and latency standards are required to compensate for clock errors in the GPS satellites. If the data latency is beyond a few seconds, the GPS clocks will have drifted sufficiently that users cannot make the corrections needed to meet the 10–20 cm requirement. Therefore, continuous high-rate data from the network are essential for real-time global differential positioning systems.

The burst impact was detected in real time (within 1 s) by the Global Differential GPS (GDGPS) system operated by NASA's Jet Propulsion Laboratory (JPL). Tracking was interrupted for many receivers that generate real-time corrections for users. The GDGPS corrections for satellites within the SRB affected service volume were unavailable for several minutes. The SRB not only affected individual receivers but prevented GDGPS from generating corrections for certain satellites. GDGPS computes corrections to the GPS satellite orbits and clocks on a continuous basis at a cadence of 1 Hz. The corrections are sent to users to improve on the direct GPS signals they acquire on their own receivers. The wide footprint of the SRB, affecting all sunlit receivers, caused certain satellites to be so poorly observed by the global network that the clock corrections could not be computed for those GPS satellites for several minutes. Automated integrity checking within the system caused a loss of corrections for users tracking certain GPS satellites. Without corrections to sufficient satellites in view, positioning accuracy for users degraded or was not even possible using the system. ... During the event, NASA/JPL's GDGPS system detected anomalous conditions, although the cause was not immediately known. Some users were immediately notified. It was later discovered that certain users were significantly affected. Significant economic impact would have resulted had the burst lasted longer, since users would have been required to operate in standby mode and suspend certain operations.

Acronyms: MHz: megahertz ; GHz: gigahertz ; sfu: solar flux units ; C/N_0 : Carrier-to-Noise ratio ; L1 : GPS frequency (1575.42 MHz) ; dB: decibel ($=10 \log_{10} (\text{Power}/\text{Power}_{\text{base}})$) ; IGS: International GNSS service ; WAAS: Wide Area Augmentation Service

GNSS impacts from solar flares

- From radio emission
 - Impact threshold
 - 1000 – 10.000 sfu
 - Not f(SXR intensity)!
 - Sunlit side ; SC minimum
 - Frequency occurrence
 - > 1000 sfu: ~ 8/year
 - > 100.000 sfu: ~ 2/year
 - Degrading eff.: ~ 9/SC



13

SXR: soft x-ray ; SC: solar cycle ; eff. Effect ; MHz: megahertz



Yue et al. , 2018 - The Effect of Solar Radio Bursts on GNSS Signals

<https://doi.org/10.1016/B978-0-12-812700-1.00022-4> (Figure 2)

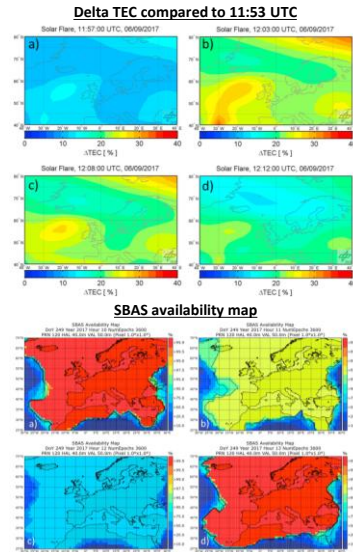
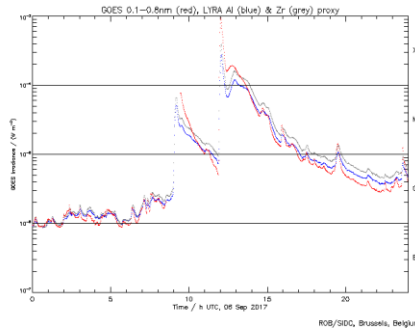
SRBs will mainly affect the stations located in the sunlit hemisphere during radio flux enhancement, while the influence strength depends on the solar incidence angle, antenna pattern, tracking algorithm, and some other factors. ... The SRB occurrence does not really depend on the intensity of solar flares. The threshold value SRB flux that could result in visible effect on GNSS signals is believed to be between 1000 and 10.000 sfu in the L-band. During 2003-12, there were 8 SRB events that showed degrading effects on GNSS signals in the literature, which is 8.8 per solar cycle. ... Significant SRBs could occur during solar minimum.

Please note that the intensities of the various radio frequencies as observed by USAF's Radio Solar Telescope Network (RSTN) are saturated at different values. For the observed frequency at 1415 MHz , this saturation level is at 100.000 sfu (Giersch et al. 2017 - <https://doi.org/10.1002/2017SW001658>). Typical undisturbed values for this frequency during solar cycle minimum and maximum are resp. 50 and 100-150 sfu.

There have been 3 strong radio emission events (at GNSS frequencies) so far this solar cycle: Any effects from the 4 May 2023 radio burst (26.000 pfu), as well as from the 2 strongest bursts so far this solar cycle on 28 August 2022 (230.000 sfu, but saturation effects?) and on 13 June 2022 (98.000 sfu by San Vito (Italy) at 1415 MHz; 64.000 sfu by Nobeyama (Japan) at 1 GHz) are thought to be much smaller and of much shorter duration than the 2006 event, and are currently being scrutinized. See this STCE newsitem at <https://www.stce.be/news/644/welcome.html> , as well as a paper by Wright et al. (2023 - <https://doi.org/10.1051/swsc/2023027> on the 28 August 2022 event reporting a fading of 13 dB at GPS L2 frequency.

GNSS impacts from solar flares

- From SXR/EUV emission
 - 6 Sep 2017: X9.3
 - Deviations up to 2m
 - Short-lived



EGNOS: European Geostationary Navigation Overlay Service ; SXR: soft x-ray ; EUV: extreme ultraviolet ; TEC: Total electron content ; SBAS: Satellite Based Augmentation System

PROBA2/LYRA: <https://proba2.sidc.be/ssa?date=2017-09-06>

Berdermann et al., 2018 - Ionospheric Response to the X9.3 Flare on 6 September 2017 and Its Implication for Navigation Services Over Europe

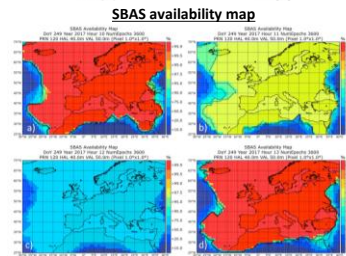
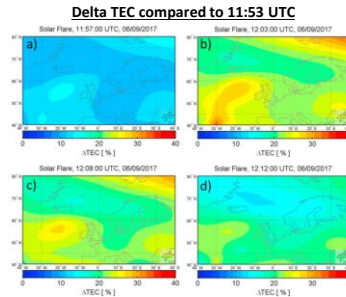
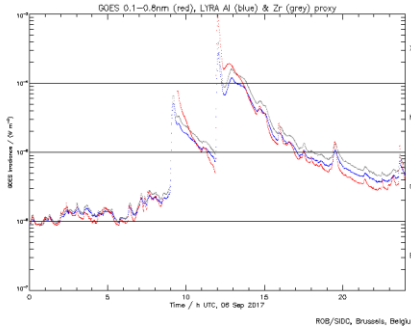
<https://doi.org/10.1029/2018SW001933> – Figures 3 and 8

Figure 3 (top right): Direct impact of the X9.3 flare on the ionosphere using the difference between the real-time assimilated TEC map over Europe and the last TEC map before the flare, which is the TEC map produced at 11.53 UTC. TEC = Total Electron Content

Figure 8 (bottom right): The hourly European Geostationary Navigation Overlay Service availability plots between 10:00 and 13:00 UT on 6 September are shown. The plots are generated with the ESA/UPC GNSS-Lab Tool (Sanz et al., 2012) and gracefully provided by ESA. Note in this figure red indicates high availability rates and blue indicates low availability rates. SBAS = satellite-based augmentation system.

GNSS impacts from solar flares

- From SXR/EUV emission
 - 6 Sep 2017: X9.3
 - Deviations up to 2m
 - Short-lived



ROB/SID, Brussels, Belgium
 EGNOS: European Geostationary Navigation Overlay Service ; SXR: soft x-ray ; EUV: extreme ultraviolet ; TEC: Total electron content ; SBAS: Satellite Based Augmentation System

Credits: Berdermann et al. (2018)

PROBA2/LYRA: <https://proba2.sidc.be/ssa?date=2017-09-06>

Berdermann et al., 2018 - Ionospheric Response to the X9.3 Flare on 6 September 2017 and Its Implication for Navigation Services Over Europe
<https://doi.org/10.1029/2018SW001933> – Figures 3 and 8

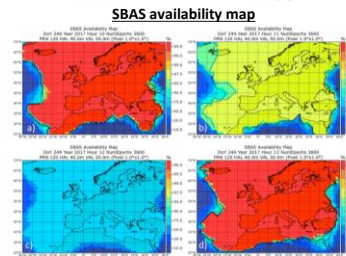
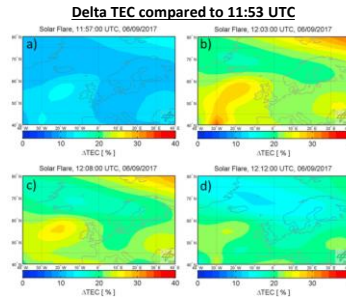
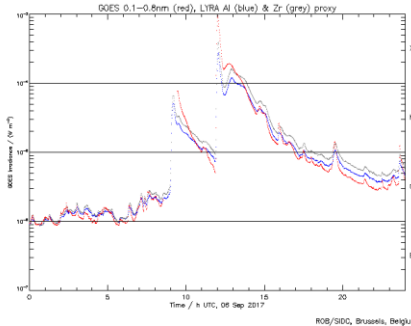
The main phase, starting around 6:00 UT on 6 September and lasting till 18:00 UT on 10 September, contains two major flare events on 6 September, an X2.2 at 9:10 UT and an X9.3 at 11:53 UT as well as strong radio burst activity over a wide range of the frequency spectrum. ... signals propagate within the Earth-ionosphere waveguide, they contain valuable information about the dynamic bottomside ionosphere, which is disturbed during solar X-ray flares (Wenzel et al., 2016). Therewith, VLF measurements by Global Ionospheric Flare Detection System complement X-ray measurements by GOES, providing information about cause and effect on the ionosphere system. So for both flares, the lower dayside ionosphere experienced an immediate response (a so-called sudden ionospheric disturbance) caused by the enhanced X-ray flux during solar flares. ... The EUV measurements by SDO illustrate a strong impact for 30.4 nm, primarily ionizing the F region (Handzo et al., 2014). Thus, a direct impact on GNSS measurements is expected.

The strongest flare event started on 6 September 2017 at 11:53 UT and ended at 12:10 with the maximum at 12:02 UT. The flare had a magnitude of X9.3 making it number 14 in the ranking of all flares observed by GOES so far. The last X-class flare of this order of magnitude occurred on 5 December 2006 more than a decade ago. The X9.3 flare had a strong effect on the ionosphere over the Central European region where the impact occurred about 2 P.M. CEST.

In Figures 3a–3d the difference between the real-time assimilated TEC maps in 5-min time steps and the TEC map just before the flare produced at 11.53 UTC is shown as reference. It becomes visible how the additional radiation component of the flare is producing a sudden increase in TEC within a very short time interval (from Figure 3a to 3b), which is decreasing after 12:03 UT (from Figure 3b to 3d). This could be seen as an indication that the additional ionospheric plasma generation due to the flare is caused in the lower layers of the ionosphere, where strong recombination processes occur, thus supporting the sudden decrease of ionospheric plasma after the flare event.

GNSS impacts from solar flares

- From SXR/EUV emission
 - 6 Sep 2017: X9.3
 - Deviations up to 2m
 - Short-lived



EGNOS: European Geostationary Navigation Overlay Service ; SXR: soft x-ray ; EUV: extreme ultraviolet ; TEC: Total electron content ; SBAS: Satellite Based Augmentation System

Credits: Berdermann et al. (2018)

PROBA2/LYRA: <https://proba2.sidc.be/ssa?date=2017-09-06>

Berdermann et al., 2018 - Ionospheric Response to the X9.3 Flare on 6 September 2017 and Its Implication for Navigation Services Over Europe
<https://doi.org/10.1029/2018SW001933> – Figures 3 and 8

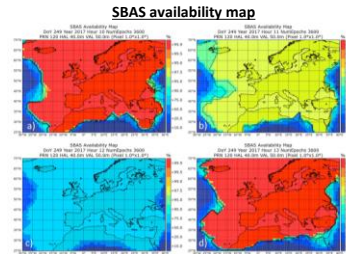
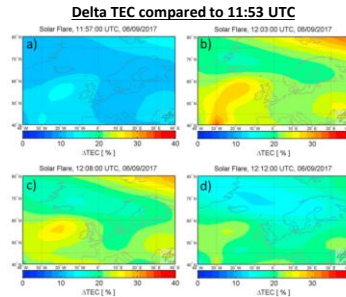
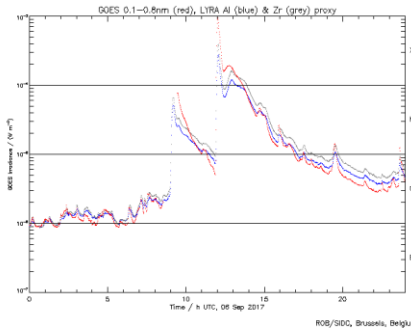
Similar observations can be made in the ROTI plots given in Figure 4. ROTI can be used as a measure to detect rapid changes of the ionospheric ionization. ROTI is calculated from real-time data stream at 1 min cadence from ground-based GNSS stations and mapped to the ionospheric pierce points. ROTI is sensitive to ionospheric perturbations and is usually used as a proxy for the S4 and $\sigma\phi$ indices derived from dual frequency high rate GNSS receiver data. S4 and $\sigma\phi$ indices describing amplitude and phase fluctuation of the received signal. The high resolution of ROTI allows studying the impact of the flare over Europe within 4 min. The whole dayside is affected as one can see in the sudden increase in ROTI from 11:56 till 11:59 UT. ROTI is typically used to identify small-scale ionospheric disturbances, but the flare event affects all used GNSS receivers due to the rapid change of the ionospheric conditions. Note that not the magnitude of TEC itself, but the sudden jump in TEC caused by strong changes in the ionosphere on a very short time scale causes problems for GNSS receiver, which are used for positioning, as we will see more in detail in section 3.

The VTEC plots show two time periods around 11:58 and 12:02 UT, where most links to the satellite lost lock. Both periods are connected with the flare and are perfectly in line with both peaks visible in the 30 nm EUV band range of SDO. This supports former publications stating that TEC responses are especially well correlated with solar EUV flux enhancements in the 26–34 nm wavelength range (Hernandez-Pajares et al., 2012; Le et al., 2013; Tsurutani et al., 2005). Please note that solar flares are often accompanied by solar radio burst events, which can cause a similar effect on GNSS signal tracking performance for high solar radio flux levels at L-Band frequencies (Rodriguez-Bilbao et al., 2015). However, measured solar radio burst events with effect on GNSS performance during this space weather event do not coincide with the loss of lock intervals visible in the VTEC plots of Figure 6b.

Navigation services based on the availability of timing information from multiple satellites experience a degradation in positioning accuracy... the single and dual frequency PPP [Precise Point Positioning] is strongly affected during the flare event. The dual frequency positioning solution is even worse compared to the single frequency solution. The interruption started at 12:00 UT followed by the typical long convergence time after reinitialization until nominal accuracy conditions are reached again. Within the convergence time period strong deviations of the estimated position in East, North, and height direction of about 1 to 2 m occurred.

GNSS impacts from solar flares

- From SXR/EUV emission
 - 6 Sep 2017: X9.3
 - Deviations up to 2m
 - Short-lived



EGNOS: European Geostationary Navigation Overlay Service ; SXR: soft x-ray ; EUV: extreme ultraviolet ; TEC: Total electron content ; SBAS: Satellite Based Augmentation System

Credits: Berdermann et al. (2018)

PROBA2/LYRA: <https://proba2.sidc.be/ssa?date=2017-09-06>

Berdermann et al., 2018 - Ionospheric Response to the X9.3 Flare on 6 September 2017 and Its Implication for Navigation Services Over Europe
<https://doi.org/10.1029/2018SW001933> – Figures 3 and 8

The European Geostationary Navigation Overlay Service (EGNOS) ... is the European regional satellite-based augmentation system. EGNOS provides safety of life navigation services to aviation, maritime, and land-based users. EGNOS is using GNSS measurements observed from precisely located reference stations within Europe and North Africa. During the X9.3 flare event, the EGNOS availability was significantly reduced as can be seen in the hourly EGNOS availability plots in Figures 8a–8d. Here the effect of both EUV peaks is clearly visible in the plot 8b from 11:00 till 11:59 UT caused by the first EUV peak at around 11:58 UT and in the plot Figure 8c from 12:00 to 12:59 UT with even stronger impact due to the second EUV peak at 12:02 UT leading to a strong decrease (10%) in the EGNOS availability. The availability is reduced over the full dayside region during this time to an amount, which might prevent the usage of EGNOS for safety of life applications, such as aircraft approach procedures based on localizer performance with vertical guidance,...

The monitoring and assessment of vessel traffic is an important element of safe, secure, and efficient shipping. Collision and grounding avoidance at sea requires a reliable picture of the maritime traffic situation. The global trend toward more autonomous operations affects also the maritime world with its need of advanced, robust, and reliable systems in every situation. Some developments in this respect has been done with the introduction of the Automatic Identification System (AIS). This system improves the safety at sea, makes bridge watchkeeping duties more comfortable, and enhances vessel traffic management ashore. ... During the solar flare period there are several peaks exceeding the one sigma limit. Such increased AIS messaging traffic might indicate an enhancement of navigation information messages due to GNSS tracking problems. There is still a strong excess in the data after the flare event at 12:26. The most plausible explanation for this feature is that the ionospheric disturbance causes some longer lasting effect on the AIS transponder software, since there was no special vessel with faulty equipment or other obvious failure modes in this time frame.

GNSS impacts from solar flares

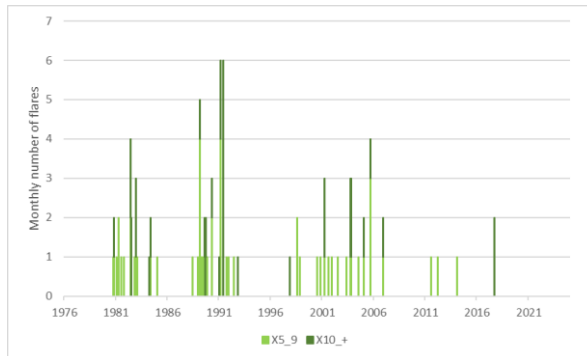
- From SXR/EUV emission

- Impact threshold

- $\sim X5$
 - $f(\text{duration})$

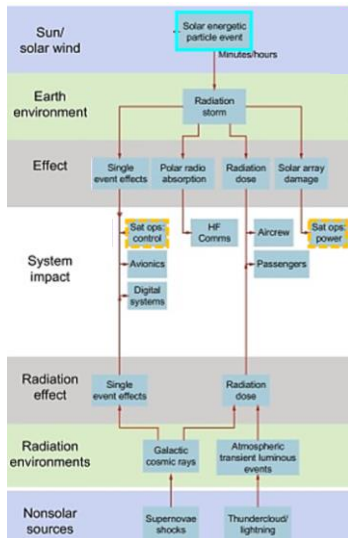
- Frequency occurrence

- $\sim 2/\text{year}$
 - Effects
 - Short-duration
 - Only sunlit side



* Note the flare values have been corrected i.a.w. guidelines by NGDC/NOAA at <https://www.ngdc.noaa.gov/stp/satellite/goes/index.html>

GNSS impacts from SEP events



• From SEP events

- Single event effects
 - *Ground Level Enhancement (GLE)*
- Polar Cap Absorption
 - Deviated by MF to poles
 - Affects D-region
 - Impacts HF Com at poles
- Radiation
 - Biological component
- Solar array damage
- Non-solar sources
 - *Supernovae (GCR)*
 - *Thundercloud lightning (TLE)*
 - South Atlantic Anomaly (LEO)

19 SEP: Solar Energetic Particles ; GCR: Galactic Cosmic Rays ; GNSS: Global Navigation Satellite Systems ; TLE: Transient Luminous Events ; MF: Magnetic field ; LEO: Low Earth Orbit ; HF Com: High Frequency Communication



Non-solar sources

- Supernovae and Black Hole activity contribute to the Galactic Cosmic Rays (GCR), a continuous low flux of highly energetic particles (think several GeV) that penetrates into the solar system. The effects are similar to the ordinary SEP events. The stream is solar cycle modulated, with the highest numbers of GCR during the solar cycle minimum and during weak solar cycles. See <https://www.stce.be/content/sc25-tracking#cosmicrays> for an example graph and <https://www.stce.be/news/433/welcome.html> for more information. See also the SPENVIS page at <https://www.spenvis.oma.be/help/background/gcr/gcr.html>
- Severe thundercloud lightning may sometimes be accompanied by Transient Luminous Events (TLE) , such as Blue Jets, Sprites, Elves,... It has been shown these TLEs may cause some ionospheric scintillation. See e.g. <https://commons.erau.edu/cgi/viewcontent.cgi?article=1028&context=db-srs>
- The South Atlantic Anomaly is an extension of Earth's inner radiation belt that is getting closer to the Earth surface. It affects only satellites in Low Earth Orbits (LEO).

GNSS impacts from SEP events

- Single Event Effects (SEE)
 - Direct hit of an electronic component by an energetic particle resulting in an anomaly
 - Phantom commands, attitude control systems, satellite failure,...
 - Several variations
 - SEU (bit flip), SEL, SEB,...
 - Frequency
 - SEP events (≥ 10 MeV): ~ 6 / year
 - Influence GCR
 - GLE events: ~ 1 / year
 - SEPs ~ 500 MeV / nucleon
 - Software glitches, medical devices,...
 - 1972 event or worse:
 - ~ 1 / 30 years

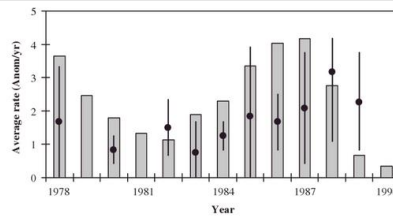
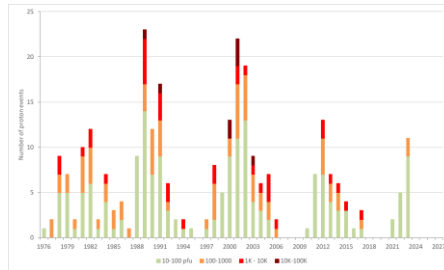


Fig. 2.5. Satellite anomaly rates for satellites in geosynchronous Earth orbit listed in the NGDC anomaly archive. The reference histogram is the annual cosmic ray flux at climax, re-scaled to show phase. (From Odenwald, 2009.)

Credits: Odenwald 2013

20 SEP: Solar Energetic Particles ; GLE: Ground Level Enhancement ; GCR: Galactic Cosmic Rays ; NGDC: National Geophysical Data Center ; SEU: Single Event Upset ; SEL: Single Event Latchups ; Single Event Burnout



Lower right figure from:

Odenwald 2013: Heliophysics: Space Storms and Radiation: Causes and Effects , pp. 15 - 42

DOI: <https://doi.org/10.1017/CBO9781139194532.003> (Figure 2.5)

Galvan et al. (2014): Satellite Anomalies

http://www.rand.org/content/dam/rand/pubs/research_reports/RR500/RR560/RAND_RR560.pdf

Single Event Effects (SEEs) - SEEs are anomalies caused not by a gradual buildup of charge over time as with surface or internal charging, but by the impact of a single high-energy charged particle into sensitive electronic components of a satellite subsystem, this single event causing ionization and an anomaly. They typically occur because of high-energy (> 2 MeV) protons and electrons striking memory devices in the spacecraft's electronics systems, causing the spacecraft (or a subsystem) to halt operations, either temporarily or permanently (e.g., Speich and Poppe, 2000). SEEs include "bit flips" or SEUs, where a high-energy particle imparts its charge to a solid-state memory device, causing errors in the system software, which may or may not damage hardware and can potentially be detected and repaired with error-detection-and-correction algorithms (EDACs) in the system software. One example of an EDAC is triple-modular redundancy (TMR), in which three processors perform the same calculations in parallel and then compare their answers. If one processor's answers differ from those of the other two, the "correct" two would outvote the incorrect one, and the third processor system could be rebooted or otherwise corrected, and the subsystem in general continues to operate. Other types of SEEs include single-event latchups (SELs), in which a subsystem hangs/crashes as a result of a high-energy particle impact. This causes the subsystem to draw excess current from the power supply, and the device must be turned off and then back on to be operable. Sometimes SEL can lead to destruction of the device if the excess drawn current is too high for the power supply. In this case, the SEE is referred to as single-event burnout (SEB, e.g., Wertz and Larson, 1999). Susceptibility to SEEs depends strongly on system design, and the risk is higher for satellites spending time in the Van Allen radiation belts or at GEO where there is a higher fluence of galactic cosmic rays and high-energy protons from Solar Proton Events (e.g., Mikaelian, 2001; Wertz and Larson, 1999);.

A good overview of the various SEE is in

Autran and Munteanu (2015) : Soft errors: from particles to circuits

https://www.researchgate.net/publication/274192779_Soft_Errors_From_Particles_to_Circuits (Fig. 1.1)

GNSS impacts from SEP events

- Single Event Effects (SEE)
 - Direct hit of an electronic component by an energetic particle resulting in an anomaly
 - Phantom commands, attitude control systems, satellite failure,...
 - Several variations
 - SEU (bit flip), SEL, SEB,...
 - Frequency
 - SEP events (≥ 10 MeV): ~ 6 / year
 - Influence GCR
 - GLE events: ~ 1 / year
 - SEPs ~ 500 MeV / nucleon
 - Software glitches, medical devices,...
 - 1972 event or worse:
 - ~ 1 / 30 years

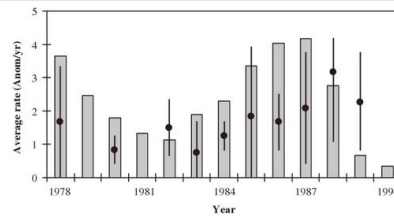
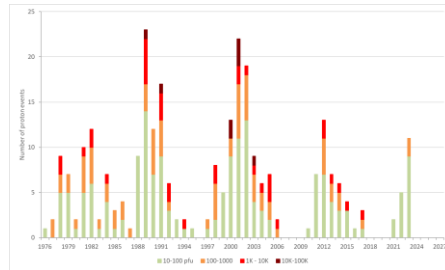


Fig. 2.5. Satellite anomaly rates for satellites in geosynchronous Earth orbit listed in the NGDC anomaly archive. The reference histogram is the annual cosmic ray flux at climax, re-scaled to show phase. (From Odenwald, 2009.)

21 SEP: Solar Energetic Particles ; GLE: Ground Level Enhancement ; GCR: Galactic Cosmic Rays ; NGDC: National Geophysical Data Center ; SEU: Single Event Upset ; SEL: Single Event Latchups ; Single Event Burnout



Credits: Odenwald 2013

Odenwald, 2013: Introduction to space storms and radiation

In: Heliophysics: Space storms and radiation: Causes and effects - <https://doi.org/10.1017/CBO9781139194532>

2.5.2 Energetic particles and solar proton events

Energetic protons (solar proton events: SPEs) are also a cause of satellite anomalies, in particular those identified as single-event upsets or SEUs. According to Brekke (2004), the solid-state recorder of the Solar and Heliospheric Observatory (SOHO) also records SEU events as memory bit-flips, which are corrected by error detection and correction (EDAC) algorithms, and the SEU counter is periodically monitored and reset. During the 1996-2003 period, a clear indication of cosmic-ray correlation found with an amplitude of 1 SEU/minute near solar minimum and 0.5 SEU/minute near solar maximum. SPEs also produce a clear and consistent signal in the SEU frequencies, typically increasing the SEU rates up to 60 SEU/min for the strongest events (e.g. the Bastille Day Storm Of July 14, 2000). For 1996-2003, three events caused SOHO to enter spacecraft safe mode, causing major disruptions of science operations. There were five events when battery discharge regulators went off-line, and seven events in which science instrument boxes were switched off. SEUs also affect the attitude control and pointing system, which employs a star tracker.

Space weather conditions can generate thousands of ESDs and SEUs in a satellite each year. The vast majority of these events go unnoticed by satellite operators and lead only to annoying data glitches (harmlessly removed by software) or momentary spikes in a particular satellite housekeeping parameter that do not exceed pre-set operational limits and are ignored as well. Occasionally, an ESD or SEU can lead to an actual operational anomaly in the satellite (phantom commands, etc.) requiring operator intervention.

The problem with both ESD and SEU related anomalies is that the event rates for both categories are extremely large and often exceed 1000 events per satellite per year. ... This larger flux (mostly galactic cosmic rays) can plausibly be modeled once specific environmental and satellite parameters are specified. However, as we see in Fig. 2.5. even the most common and non-critical satellite anomalies only represent 1-2 events per satellite per year. At this rate, the mean time to failure is about 200 years per satellite for an anomaly that proves fatal.

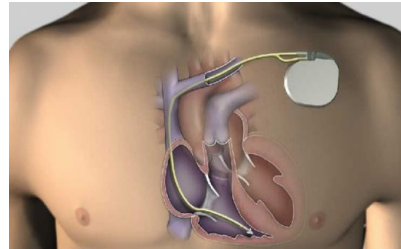
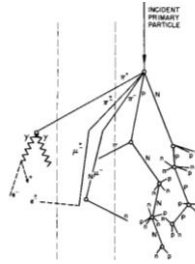
2.6 How bad can it get?

Satellite designers use sophisticated tools to assess radiation hazards under worst case conditions (e.g. the August 1972 and March 1991 events). However, studies of extreme space weather conditions suggest that the period since 1960 may not be typical.

According to McCracken et al. (2001) and Townsend et al. (2006), the 1859 storm was the most extreme event observed in the last 500 years, ... This fluence is about four times greater than the canonical worst-case August 4, 1972, event, which was the strongest solar event during the satellite era. Since 1561, there have been 19 SPEs more intense than the August 1972 SPE (approximately one every 30 years). Nevertheless, a once-a-century or once-a-millennium superstorm would be a disaster to our satellite resources, and its probability of occurrence is far higher than other risks, such as the next San Francisco earthquake, which are taken more seriously.

GNSS impacts from SEP events

- Ground Level Enhancement (GLE)
 - Sharp increase of #neutrons at ground
 - Main source
 - Strong SEPs ~500 MeV per nucleon
 - => RARE!!
 - Only 73 GLEs since the 1940s
 - GLE#73: 28 Oct 2021
 - Strongest GLE
 - 23 Feb 1956
 - Impacts
 - Computer glitches, servers,...
 - Errors increase with altitude
 - Pacemakers, defibrillators, and other medical devices,...
 - SEUs (very low rates)



SEP: Solar Energetic Particles ; GLE: Ground Level Enhancement ; GCR: Galactic Cosmic Rays ; MeV: mega electronvolt ; SEU: Single Event Upset



Top right figure taken from Wikimedia Commons (NGDC/NOAA):
<https://www.ngdc.noaa.gov/stp/image/shower.gif>

Thakur et al. (2014): Ground Level Enhancement in the 2014 January 6 Solar Energetic Particle Event
<https://ui.adsabs.harvard.edu/abs/2014ApJ...790L..13T/abstract>
Solar energetic particle (SEP) events, where particles accelerated to GeV energies are subsequently detected on the ground as a result of the air-shower process, are known as ground level enhancements (GLEs). With a typical detection rate of a dozen GLEs per cycle, an average of 16.3% SEP events were GLEs in cycles 19–23 (Cliver et al. 1982; Cliver 2006; Shea & Smart 2008; Mewaldt et al. 2012; Nitta et al. 2012; Gopalswamy et al. 2012a). In cycle 24, this fraction is much smaller (6.4%) with 2 GLEs out of 31 large SEP events (Gopalswamy et al. 2014). This is also much smaller than the ratio of 18% obtained when the first five years of cycle 23 are considered. GLEs are typically associated with intense flares (median soft X-ray intensity $\sim X3.8$) and fast coronal mass ejections (CMEs; average CME speed ~ 2000 km s $^{-1}$; see Gopalswamy et al. 2012a).

Usoskin et al. (2016): Database of Ground Level Enhancements (GLE) of High Energy Solar Proton Events
<https://pos.sissa.it/236/054>

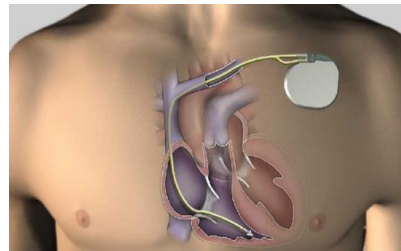
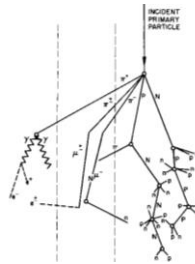
From the Royal Academy of Engineering (2013)
https://raeng.org.uk/media/lz2fs5ql/space_weather_full_report_final.pdf

9.3 Engineering consequences of an extreme event on ground systems

The atmosphere provides considerable protection to ground level systems and for this reason this study focuses on airborne systems. Yet we know that SEEs are occasionally seen on ground systems [normand, 1996; Ziegler et al., 1996] and are likely to be of increasing concern in the design of automotive electronics, miniaturised devices and safety-critical systems in general. Medical devices such as implantable cardiac defibrillators have been shown to give errors from cosmic rays [bradley and normand, 1994].

GNSS impacts from SEP events

- Ground Level Enhancement (GLE)
 - Sharp increase of #neutrons at ground
 - Main source
 - Strong SEPs ~500 MeV per nucleon
 - => RARE!!
 - Only 73 GLEs since the 1940s
 - GLE#73: 28 Oct 2021
 - Strongest GLE
 - 23 Feb 1956
 - Impacts
 - Computer glitches, servers,...
 - Errors increase with altitude
 - Pacemakers, defibrillators, and other medical devices,...
 - SEUs (very low rates)



SEP: Solar Energetic Particles ; GLE: Ground Level Enhancement ; GCR: Galactic Cosmic Rays ; MeV: mega electronvolt ; SEU: Single Event Upset



Upsets in major computing facilities correlate with altitude and, since a major server suffered significant outages and caused economic losses, certain server technologies have been tested in neutron radiation facilities [Lyons, 2000]. In light of this evidence, safety-critical ground systems such as those in nuclear power stations should consider the impact of superstorm radiation at ground level within its electronic system reliability - and safety assessments. In the case of nuclear power a Carrington event may not be a sufficient case since relevant timescales for risk assessment may be as long as 10,000 years.

10.4 GNSS - summary and recommendations

Assuming that the satellites – or enough of them – survive the impact of high energy particles, we anticipate that a solar superstorm will render GNSS partially or completely inoperable for between one and three days. The outage period will be dependent on the service requirements. For critical timing infrastructure, it is important that holdover oscillators be deployed capable of maintaining the requisite performance for these periods. UK networked communications appear to meet this requirement. With current forecast skills, it is inevitable that aircraft will be flying and ships will be in transit when the superstorm initiated. Aircraft use differential and augmented systems for navigation and in the future possibly for landing. With these applications set to increase, the potential for significant impact from an extreme space weather event will likewise increase. Fortunately, the aviation industry is highly safety conscious and standard operating procedures appropriate to other emergency situations are likely to provide sufficient mitigation to an extreme space weather event. These include other terrestrially based navigation systems. The challenge will be to maintain those strategies over the long term as GNSS become further bedded into operations.

- Pacemaker incident

BBC: <https://www.bbc.com/future/article/20221011-how-space-weather-causes-computer-errors>

- Bradley et al. (1998): Single Event Upsets in Implantable Cardioverter Defibrillators

<http://cardiacos.net/wp-content/uploads/ArticulosMedicos/20170707/1994---Single-Event-Upsets-in-Implantable-Cardioverter-Defibrillators.pdf>

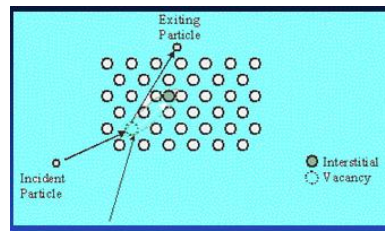
Also at http://www.iaea.org/inis/collection/NCLCollectionStore/_Public/29/003/29003514.pdf

- Normand (2013): Single Event Upset at Ground Level

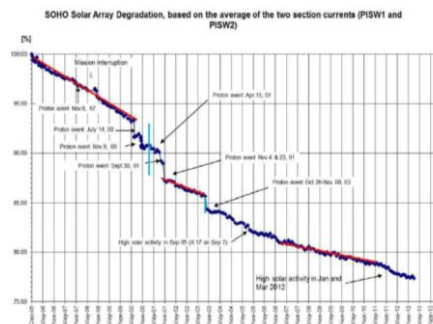
<https://web.archive.org/web/20131021190327/http://pdf.yuri.se/files/art/2.pdf>

GNSS impacts from SEP events

- Solar array damage
 - Displacement damage
 - Reduces efficiency in electricity production
 - Several % loss from one proton event is possible
 - 2% loss during Bastille Day event (14 July 00)
 - 5% loss during extreme 4 August 1972 event
- Overall aging process of satellite and its instruments
 - Galactic Cosmic Rays



Credits: Valtonen 2004



Credits: Curdt et al. 2015

24

Top figure taken from Valtonen (2004): Space Weather: Effects on Space Technology
<http://slideplayer.com/slide/3603908/> (slide 33)

Bottom figure taken from Curdt et al. (2015): Solar and Galactic Cosmic Rays Observed by SOHO
<https://ui.adsabs.harvard.edu/abs/2015CEAB...39..109C/abstract> (Figure 5)

Fig. 5 shows the degradation of the solar array efficiency from Dec 1995 until Feb 2013. The total loss was ~22.5% during that time (and has reached 24% at the end of 2014). The degradation starts with a linear, continuous decrease of 0.00368% / d (1.344% per year) from launch to Jul 2000. We attribute this decrease to the CRF (Cosmic Ray Flux) during SOHO's first solar minimum. Then follows a phase of several stepwise decrements that can be associated to SEP events during the maximum of cycle 23 around 2001. Here, individual proton events start to dominate the scene. Later follow two more episodes with continuous - but less steep - decrease. Around 2002, the degradation rate is 0.00284% / d (from a starting point of 87.2%) and only 0.00168% / d (from a starting point of 82.1%) during the period from Feb 2007 to May 2011. There is no evidence for a significant solar cycle variation. It seems as if a continuous decrease of the degradation rate reduces the value by almost a factor of two. ... We speculate that in the solar arrays cells of different radiation hardness are found and that destruction of less-radiation hard cells is in progress all the time. Also, ageing effects of the cover-glass could be responsible for efficiency loss. We tried to quantify the effects of cosmic rays and the effects of SEPs during this period. In total, of the 22.5% power loss 8.5% can be attributed to proton events. Hereof, 5% occurred during a period of only 1.5 years. Altogether, 38% ± 2% of the degradation during 17 years can be attributed to proton events. In other words: the effect of a series of violent short-term events on the solar panels is comparable to the accumulated effect of the CRF over this period. [Note SOHO is located outside the Earth's magnetosphere, in the Lagrange 1 point].

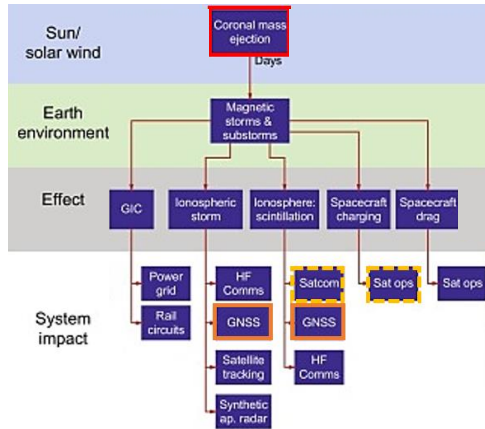
Another nice example of solar array degradation is in Hubner et al. (2012): INTEGRAL revisits Earth - Low perigee effects on spacecraft components
<http://arc.aiaa.org/doi/abs/10.2514/6.2012-1291272>

Some interesting statistics on solar array degradation provided by Intelsat:
<http://www.intelsat.com/tools-resources/library/satellite-101/space-weather/>

D. Knipp: On the Little-Known Consequences of the 4 August 1972 Ultra-Fast Coronal Mass Ejecta: Facts, Commentary, and Call
<https://agupubs.onlinelibrary.wiley.com/doi/full/10.1029/2018SW002024>

Rauschenbach (1980) showed an ~5% drop in solar cell power generation capability for the INTEL SAT IV F-2 [a geostationary satellite] solar panel arrays during the 4 August SEP event, roughly equivalent to 2 years of magnetospheric trapped-radiation exposure to the panels.

GNSS impacts from ICMEs



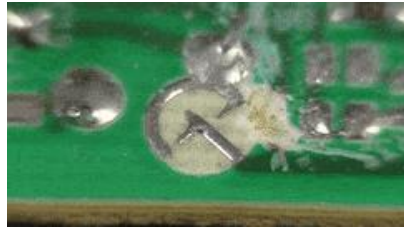
- From magnetic field
 - Satellites
 - Magnetopause crossings
 - High-Precision industry
 - GCR: Forbush decrease
- From particles
 - Satellites
 - Drag
 - Charging effects
 - Satellite-based Comms/Nav applications (GNSS)
 - HF Communication (aviation)
 - Geomagnetically Induced Currents (GIC)
 - Aurora

GCR: Galactic Cosmic Rays ; Comms/Nav: Communications/Navigation ;
 PECASUS: Partnership for Excellence in Civil Aviation Space weather User
 Services ; HF: High Frequency ; (ICME): (Interplanetary) Coronal Mass Ejection



GNSS impacts from ICMEs

- Charging effects
 - Surface charging
 - Low energy plasma
 - $\sim 10\text{-}50$ keV electrons
 - Substorm related
 - SWPC: likely if $K \geq 6$
 - Electrostatic discharge (ESD)
 - Surface damage
 - Phantom commands
 - Internal charging
 - $\sim 100\text{s}$ keV electrons
 - Galaxy 15 outage in April 2010
 - Accumulation effect



Credits: eevblog.com

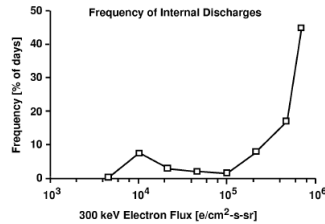


Figure 11. Comparison of SCATHA anomalies with energetic electron fluxes.

Credits: Fennell et al. (2001)

26

Top right figure: Spark gap gif from <https://www.eevblog.com/2014/10/31/eevblog-678-what-is-a-pcb-spark-gap/>
 Bottom right figure:

Fennell et al. (2001): Spacecraft Charging: Observations and Relationship to Satellite Anomalies
<https://ui.adsabs.harvard.edu/abs/2001ESASP.476..279F/abstract>

Fennell et al. (2001): Spacecraft Charging: Observations and Relationship to Satellite Anomalies
<https://ui.adsabs.harvard.edu/abs/2001ESASP.476..279F/abstract>

2. Satellite Surface Charging

In the early 1970's, it became clear that many of the anomalies on geosynchronous satellites occurred in the near midnight to dawn region of the magnetosphere, as shown in Figure 1. This was reminiscent of the path that the hot substorm-injected electrons from the magnetotail take as they drift around the magnetosphere. Thus, it was thought that the anomalies might be substorm related and could be caused by satellite charging.

As we know, 10's of keV electrons do not penetrate the satellite surface materials but reside near the surface. The incident plasma and the solar UV also interact with materials to generate secondary electrons. The satellite's surface materials will take on a charge such that the net current between the surfaces and the plasma is zero under quiescent conditions. The result is that the surface voltages would not be zero. The sunlit areas are usually slightly positive and the shadowed areas are usually negative relative to the plasma at "infinity". If the surface was a conductor, the potential of the surface would be uniform and either positive or negative relative to the plasma.

More info at

Dr Holbert - bottom image

Valtonen (2004): https://link.springer.com/chapter/10.1007/978-3-540-31534-6_8 (topleft image)

Gubby et al. (2002): Space environment effects and satellite design

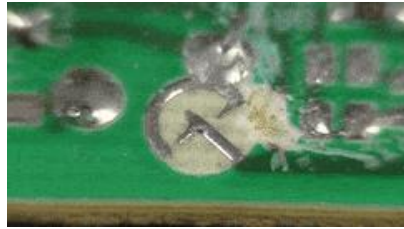
<https://ui.adsabs.harvard.edu/abs/2002JASTP..64.1723G/abstract>

The common measure for geomagnetic storms, and hence the occurrence of surface charging, is the K index. This index is a 3 hourly measure ranging from 0-9 (0=quiet, 9=severely disturbed.). It is derived from ground-based magnetometer data and is used as a surrogate for actual plasma measurements at satellite altitudes. In general, surface charging effects begin at the K=4 to K=5 level. Charging is probable at $K \geq 6$ (see Today's Space Weather). Geomagnetic substorms can be somewhat localized in space so the use of the planetary K index (K_p) may mask the severity of effect upon a specific spacecraft.

Also at STCE news item: Itchy satellites: <https://www.stce.be/news/207/welcome.html>

GNSS impacts from ICMEs

- Charging effects
 - Surface charging
 - Low energy plasma
 - $\sim 10\text{-}50$ keV electrons
 - Substorm related
 - SWPC: likely if $K \geq 6$
 - Electrostatic discharge (ESD)
 - Surface damage
 - Phantom commands
 - Internal charging
 - $\sim 100\text{s}$ keV electrons
 - Galaxy 15 outage in April 2010
 - Accumulation effect



Credits: eevblog.com

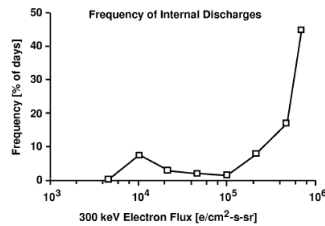


Figure 11. Comparison of SCATHA anomalies with energetic electron fluxes.

Credits: Fennell et al. (2001)

27

Denig et al. (2010): **Space Weather Conditions at the Time of the Galaxy 15 Spacecraft Anomaly**

https://www.ngdc.noaa.gov/stp/satellite/anomaly/2010_sctc/docs/1-2_WDenig.pdf

Solar activity was elevated but not remarkable. Global geomagnetic activity described by the AL auroral electrojet index and Kp were extreme. Other SWx indices were more moderate. Local measurements near Galaxy 15 show that a large geomagnetic substorm occurred 48 minutes prior to the anomaly. The substorm caused remarkable increases in the measured local flux of energetic particles known to cause surface or internal satellite charging.

[Note the Galaxy 15 was a geostationary telecommunications satellite to support the GNSS/WAAS. Ground controllers were able to regain contact and reposition the satellite in April 2011. On 10 August 2022, contact with the satellite was lost permanently following a [unspecified] SWx event (<https://www.satellitetoday.com/broadcasting/2022/08/22/intelsat-loses-command-of-galaxy-15-satellite/>)].

Internal charging: Valtonen (2004): https://link.springer.com/chapter/10.1007/978-3-540-31534-6_8

Another example of internal charging by CME is the Telstar-401 (11 January 1997):

Odenwald: <http://www.solarstorms.org/SWChapter2.html>

<http://sdoisgo.blogspot.be/2016/06/telstar-401-ghost-of-space-weather-past.html>

A less clear example (based more on circumstantial evidence) was the failure of the Galaxy-IV satellite, more than a week after the passage of several strong CMEs that even created a third radiation belt. The official report mentioned only technical causes, no link to the geomagnetic storms.

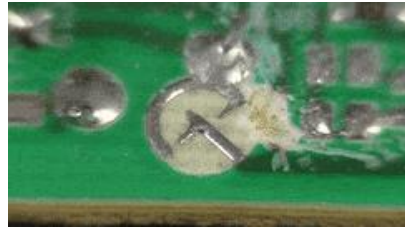
NASA: <https://pwg.gsfc.nasa.gov/istp/outreach/events/98/>

SPACECAST: http://fp7-spacecast.eu/help/bg_sa.pdf

Also at SWS: <http://www.sws.bom.gov.au/Educational/1/3/2> : **Satellite Communications and Space Weather**

GNSS impacts from ICMEs

- Charging effects
 - Surface charging
 - Low energy plasma
 - $\sim 10\text{-}50$ keV electrons
 - Substorm related
 - SWPC: likely if $K \geq 6$
 - Electrostatic discharge (ESD)
 - Surface damage
 - Phantom commands
 - Internal charging
 - $\sim 100\text{s}$ keV electrons
 - Galaxy 15 outage in April 2010
 - Accumulation effect



Credits: eevblog.com

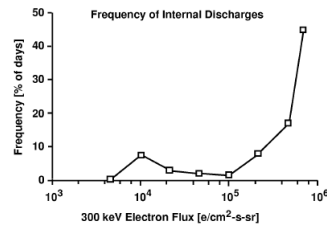


Figure 11. Comparison of SCATHA anomalies with energetic electron fluxes.

Credits: Fennell et al. (2001)

28

Mateo-Velez, 2017: Spacecraft surface charging induced by severe environments at geosynchronous orbit

<https://doi.org/10.1002/2017SW001689>

Extreme spacecraft charging conditions of the order of 10 kV were first recorded by geosynchronous satellites ATS 5 and ATS 6 (DeForest, 1972, 1973). It was shown that most of severe charging events were measured during eclipse and high Kp index (Garrett, 1981). Surface charging is the result of a complex interaction between the spacecraft and its plasma environment (e.g., Lai, 2012). At GEO in eclipse, the main contribution to spacecraft potential is the ambient electron current, especially during electron flux enhancement by geomagnetic storms and sub-storms. At GEO in sunlight, the largest contribution to spacecraft potential is the emission of electron by UV photon impacts.

Even though the occurrence rate of the higher Kp indexes (6–9) over the 16 years reaches about 2%, they are related to a much higher percentage of the charging events (74/400). This is consistent with prior studies that showed a consistent up trend of frame potential with higher Kp (Garrett, 1981). 82 events out of 100 occurred in eclipse and lasted less than the eclipse duration. ... These results clearly confirm that the response of a spacecraft to the space environment is very different in sunlight and in eclipse.

Electrostatic discharges on solar panels can generate arcing between solar cells and produce power losses. Arcing on power cable harness is also a concern. For instance, the failure of the Advanced Earth Observation Satellite (ADEOS) II occurred at low altitude of 800 km in the auroral zone made very active with high flux of >30 keV electrons during the "Halloween event" on October 24, 2003 due to a Coronal Mass Ejection (Cho, 2005). The loss was attributed to power cable harness arcing (Maejima et al., 2004).

GNSS impacts from ICMEs

- Ionospheric disturbances – ICAO - GNSS

Table 1. Parameters and thresholds that are used to issue space weather advisories according to ICAO regulations.

Impact Area	Parameter (Unit)	Moderate	Severe
GNSS	Amplitude scintillation S_4 (dimensionless)	0.5	0.8
	Phase scintillation σ_ϕ (radians)	0.4	0.7
	Vertical TEC (TEC Unit)	125	175

Table 2. Criteria for alerting the PECASUS operator on duty. Based on these criteria, the operator investigates and possibly sends an advisory. The moderated thresholds are given for each data type in Table 1, respectively.

Monitored Effects	Alert for the Operator
S_4 and σ_ϕ Scintillation	Over the last 15 min, 50% of the scintillation observations recorded at one station have reached the moderated threshold.
Vertical TEC maps	A single data point anywhere on the map reached the moderated threshold.

Credits: Kauristie et al. (2021)

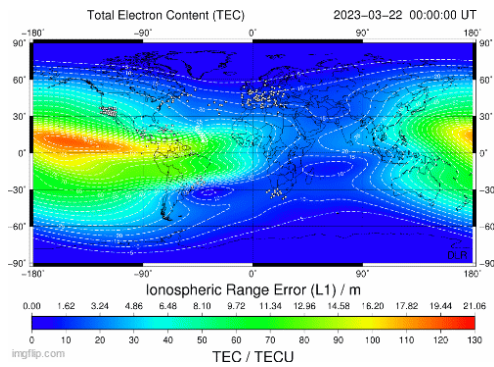
2! ICAO: International Civil Aviation Organization ; PECASUS: Partnership for Excellence in Civil Aviation Space weather User Services ; (I)CME: (Interplanetary) Coronal Mass Ejection ; (V)TEC: (Vertical) Total Electron Content ; TECU: TEC Unit



Table excerpt from Kauristie et al. (2021) - Space Weather Services for Civil Aviation – Challenges and Solutions
<https://doi.org/10.3390/rs13183685>

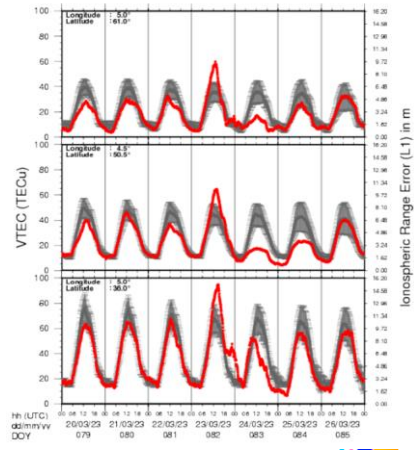
GNSS impacts from ICMEs

- Ionospheric storm
 - Example: 23-24 Mar 2023
 - $K_p = 8.0$; $Dst = -163$ nT



30

Credits images: PECASUS & DLR/IMPC

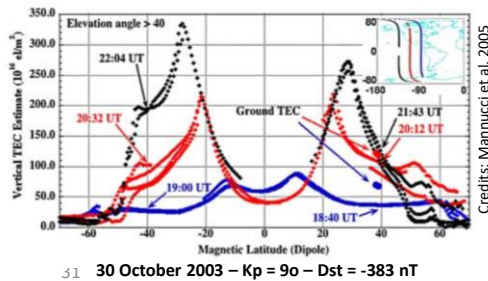


<https://www.stce.be/news/640/welcome.html>

<https://www.stce.be/news/638/welcome.html>

GNSS impacts from ICMEs

- Ionospheric storm
 - VTEC based
 - Local values
 - Geomagnetic storms in March and April 2023
 - $VTEC_{max} \sim 170 \text{ TECu}$; Dst resp. -163 nT and -212 nT



30 October 2003		
Kp	9o	
Dst	-383 nT	
Position repeatability	North-Europe	Central Europe
Quiet Sun (2008)	2,5 cm	2,5 cm
30 October 2003	26,1 cm	3,1 cm

Credits data: Bergeot et al. 2011



Lower-left figure from Mannucci et al. 2005 - Dayside global ionospheric response to the major interplanetary events of October 29–30, 2003 “Halloween Storms”
<https://doi.org/10.1029/2004GL021467>

Figure 3. The supersatellite integrated electron content (IEC) as measured by the CHAMP spacecraft is shown just prior (blue trace) and after (red and black traces) the onset of the interplanetary event of October 30 (see Figure 1). The different sets of points for each trace correspond to IEC measured towards the different GPS satellites at each epoch, which are all used to estimate vertical TEC directly above the CHAMP satellite altitude of 400 km, using an elevation angle cut-off of 40 degrees to reduce the error in the vertical IEC estimation procedure. The local time of the CHAMP orbit ranges from 1230–1330 LT for latitudes within ± 60 degrees. Points missing near the anomaly trough are due to the elevation angle cut-off. The universal times of the ~ 40 and $+40$ degree latitude cross-over points are shown for each trace. Also shown in the upper right are the geographical locations of the traces. Total electron content averages from ground data near to the CHAMP ground track are shown as round dots.

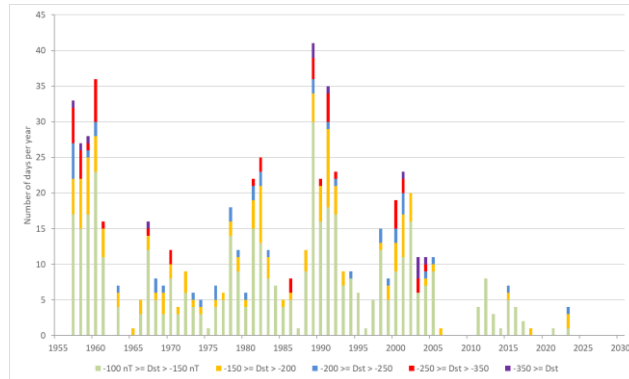
Lower-right: Data from Bergeot et al. 2011 - Impact of the Halloween 2003 ionospheric storm on kinematic GPS positioning in Europe

<https://link.springer.com/article/10.1007/s10291-010-0181-9>

In order to understand the impact of an ionospheric storm on high-precision kinematic GPS applications, we computed the position of 36 EPN stations every 5 min during the October 29–30, 2003 ionospheric storm using the commonly adopted first-order ionosphere-free combination. These 5-min positions were computed for each station separately, in a network of stations with fixed positions, and tropospheric parameters and ambiguities determined in preliminary daily processing. Under normal ionospheric conditions during solar minimum activity in 2008, the repeatability is better than 1 cm in the horizontal and close to 2.5 cm in vertical. During the Halloween storm, the position repeatability of the kinematic positions for locations in northern Europe turned out to reach 12.8, 8.1 and 26.1 cm for the North-East-Up components. For stations in central Europe, the position repeatability turned out better, i.e. in the range of 1–2 cm in the horizontal and 3.1 cm in the up component.

GNSS impacts from ICMEs

- Severe ionospheric storm frequency
 - $Dst \leq -200$ nT: 1.4 days / year ; 16 days / SC
 - $Dst \leq -250$ nT: 0.8 days / year ; 9 days / SC
 - But none since 2005...



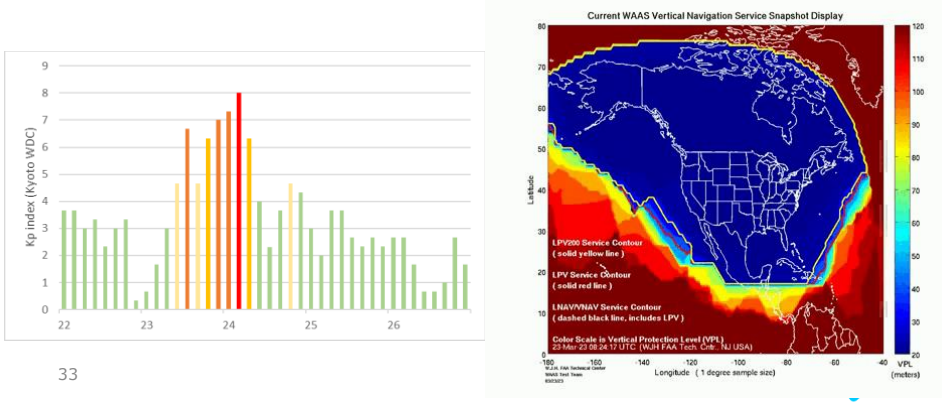
32



Data from the World Data Centre (WDC) for Geomagnetism, Kyoto, Japan
Graph from STCE – SC25 Tracking: <https://www.stce.be/content/sc25-tracking>

GNSS impacts from ICMEs

- Ionospheric scintillations
 - Example: 23-24 March 2023
 - $K_p = 8.0$; $Dst = -163$ nT



<https://www.stce.be/news/640/welcome.html>
<https://www.stce.be/news/638/welcome.html>

This daily 24-hour plot below depicts the Wide Area Augmentation System (WAAS) Lateral Precision with Vertical Guidance 200 (LPV200) service in North America. Vertical Protection Level (VPL). The Vertical Protection Level is half the length of a segment on the vertical axis (perpendicular to the horizontal plane of WGS-84 ellipsoid), with its center being at the true position, which describes the region that is assured to contain the indicated vertical position. It is based upon the error estimates provided by WAAS. LPV Service (Solid Red Line). Area encompassed meets WAAS LPV operational service level with horizontal alert limit (HAL) equal to 40 meters and a vertical alert limit (VAL) equal to 50 meters.

EGNOS LPV200 Availability is defined as the percentage of epochs which the Protection Level are below Alert Limits for this service ($HPL < 40m$ and $VPL < 35m$) over the total period. The pictures present the current EGNOS LPV200 Availability over the last 24 hours and the last hour and the corresponding VPL and HPL for the operational GEO satellites and Combined GEO satellites.

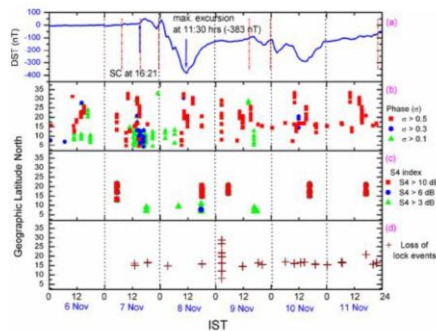
From ESWW19 (Lidia Nikitina):

7 Nov 2022: GNSS application problems (WAAS as well as EGNOS); In Canada, errors of 40 m (horizontal) and 50 meters (vertical GIVE) due to scintillation errors were recorded. CADORS (Canadian event reports) reported that one plane missed its approach landing strip and do it all over. Also, during the major geomagnetic storm of 25-27 Feb 2023, several pilots reported problems with LPV and approach navigation. Another strong WAAS disturbance was reported on 5 Nov 2023.

GNSS impacts from ICMEs

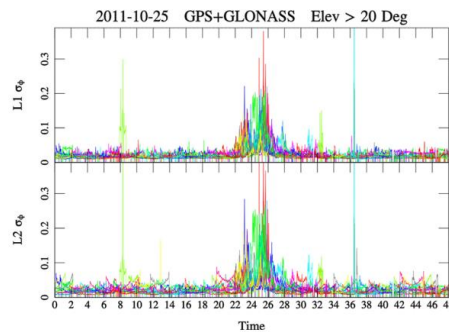
- Ionospheric scintillations

- 8 November 2004
 - Kp=9o ; Dst=-374 nT



34

- 24-25 October 2011
 - Kp=7+ ; Dst=-147 nT



Credits: Jacobsen et al. 2012



Lowerleft figure: 8 November 2004 from Rama Rao et al. 2009 - Geomagnetic storm effects on GPS based navigation

<https://doi.org/10.5194/angeo-27-2101-2009>

In Fig. 7, where the phase (σ) and amplitude (S4) indexes are presented along with the loss of lock events as a function of latitude and local time during the storm period, also shows the occurrences of phase slips for the entire period 6 to 11 November 2004, when the 8 and 10 November storms have occurred. Figure 7b shows the phase slips and the associated phase scintillation (σ) index of three different intensity levels (>10 dB, >6 dB, >3 dB) and Fig. 7c shows the phase slips that are accompanied with reduced signal-to-noise ratio as indicated by the amplitude scintillation (S4 index) at the three different power levels. Some of these phase slips, resulting in the loss of lock of the GPS receiver that are detected from the lock time of the receiver, are shown in Fig. 7d. It may also be seen from this figure that most of the slips are associated with phase (σ) index rather than with S4 index. These loss of locks are caused as a result of rapid phase fluctuations in the received signal carrier exceeding the receiver's phaselock-loop (PLL) bandwidth, and in some cases resulting in the decrease of the signal-to-noise ratio beyond the threshold value of the receiver, which may also vary from receiver to receiver. However, from the communications and navigation point of view, these loss of lock events are undesirable and need to be accounted for in an appropriate manner.

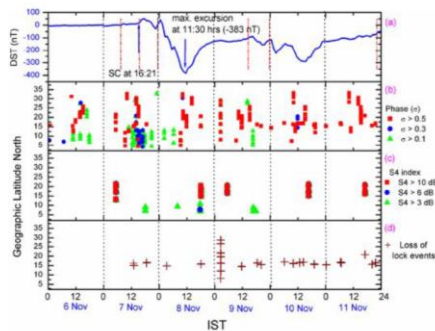
Penn State University: <https://www.e-education.psu.edu/geog862/node/1728>

A cycle slip is a discontinuity in a receiver's phase lock on a satellite's signal.

GNSS impacts from ICMEs

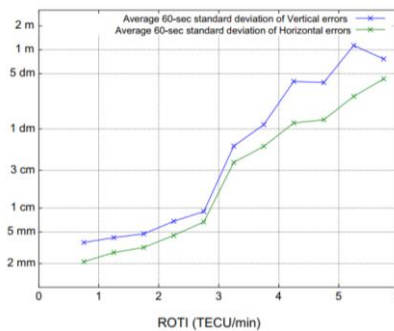
- Ionospheric scintillations

- 8 November 2004
 - Kp=9o ; Dst=-374 nT



Credits: Rama Rao et al. 2009

- 24-25 October 2011
 - Kp=7+ ; Dst=-147 nT



Credits: Jacobsen et al. 2012

35



Lower right figures in this and previous slide : 24-25 October 2011 from Jacobsen et al. 2012 - Observed effects of a geomagnetic storm on an RTK positioning network at high latitudes - <https://doi.org/10.1051/swsc/2012013>

To quantify the effects of the ionospheric disturbances on the positioning accuracy, the 60-s standard deviation of the vertical and horizontal coordinates was binned by ROTI and then averaged. The results are shown in Figure 14. The error increases exponentially with increasing ROTI values. At ROTI greater than three, the error is significantly greater than any local error source. It is noted that as this is the average level of the standard deviation of the position error, individual positions can have a far greater error. This graph shows that small-scale structuring of the ionospheric plasma has a detrimental effect on the final coordinates computed in an RTK system, even for low levels of activity. As the ionospheric activity increases, the effect grows exponentially and at high levels of ionospheric activity it becomes greater than any other error source.

Scintillation effects from 30 October 2003 also in:

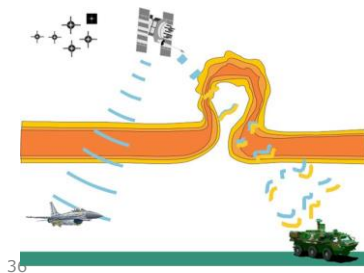
Alfonsi et al. 2006 - Positioning errors during space weather
<https://www.earth-prints.org/bitstream/2122/4035/1/40.pdf>

GNSS impacts from ICMEs

- Ionospheric scintillations

- Reminder

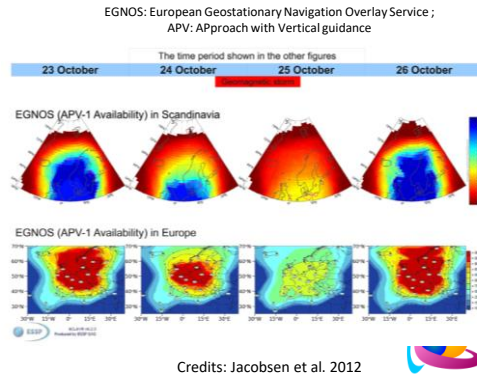
- Also when geomagnetic activity is quite low
 - Battle of Takur Ghar!
 - Satcom (2002)



Credits: US Air Force Research Laboratory

- 24-25 October 2011

- $K_p=7+$; $Dst=-147$ nT



Lower left figure from US Air Force Research Laboratory -
https://www.nasa.gov/mission_pages/cindi/five-years.html

Lower right figure from:

24-25 October 2011 from Jacobsen et al. 2012 - Observed effects of a geomagnetic storm on an RTK positioning network at high latitudes
<https://doi.org/10.1051/swsc/2012013>

An overview of the European Geostationary Navigation Overlay Service (EGNOS) (EGNOS website) performance during the storm days is shown in Figure 5. One day prior to and after the storm days have been included to show the performance during normal conditions. The time resolution of the EGNOS plots is one day. The plots show that EGNOS clearly suffered from service disruptions during the storm. The plots for the 24th October show disruptions mainly in the North, while the plots for 25th October show a disruption for the entire EGNOS area. This is consistent with the ionospheric disturbances shown in Figure 4, which indicate that for the southern latitudes, the main disturbances were seen on the 25th.

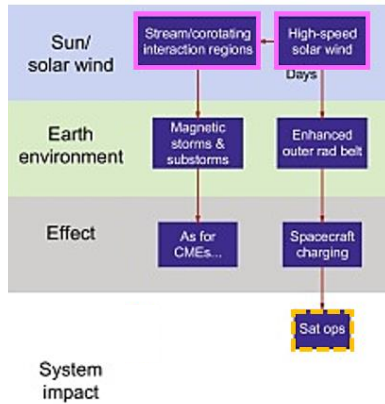
Battle of Takur Ghar (4 March 2002) - <https://www.stce.be/news/420/welcome.html>

Kelly et al. 2014 - Progress toward forecasting of space weather effects on UHF SATCOM after Operation Anaconda

<https://doi.org/10.1002/2014SW001081>

During Operation Anaconda, the Battle of Takur Ghar occurred at the summit of a 3191 m Afghan mountaintop on 4 March 2002 when the ionosphere was disturbed and could have affected UHF Satellite Communications (SATCOM). In this paper, we consider UHF SATCOM outages that occurred during repeated attempts to notify a Quick Reaction Force (QRF) on board an MH-47H Chinook to avoid a "hot" landing zone at the top of Takur Ghar. During a subsequent analysis of Operation Anaconda, these outages were attributed to poor performance of the UHF radios on the helicopters and to blockage by terrain. However, it is also possible that ionospheric anomalies together with multipath effects could have combined to decrease the signal-to-noise ratio of the communication links used by the QRF. A forensics study of Takur Ghar with data from the Global Ultraviolet Imager on the NASA Thermosphere Ionosphere Mesosphere Energetics and Dynamics mission showed the presence of ionospheric bubbles (regions of depleted electron density) along the line of sight between the Chinook and the UHF communications satellites in geostationary orbit that could have impacted communications.

GNSS impacts from CH HSS



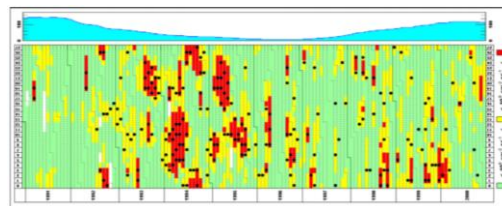
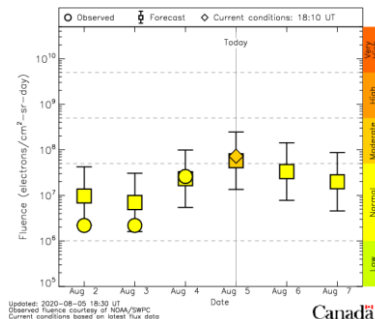
- Similar to effects from ICMEs but less intense
- except...
- From particles
 - Satellites
 - Deep di-electric charging

CH: coronal hole ; HSS: high speed stream ; (I)CME: (Interplanetary) Coronal Mass Ejection ; Sat ops: satellite operations



GNSS impacts from CH HSS

- High-Speed Stream (HSS)
 - Satellite charging
 - Deep di-electric charging
 - About 1 to few MeV e⁻
 - Deeply penetrate spacecraft (S/C)
 - Fluxes ≥ 2 MeV e⁻
 - Accumulation effect within S/C (ESD)
 - Due to day-night effect
 - Fluence (24h)
 - Declining phase solar cycle (coronal holes)
 - ~ 20 ESD/yr/GEO sat
 - Also strong ICME, e.g. 3-4 Nov 2021



#ESDs on a GEO communications satellite
Credits: Wrenn et al. (2002)

38

Bottomright figure:

Wrenn et al. (2002): A solar cycle of spacecraft anomalies due to internal charging

<https://ui.adsabs.harvard.edu/abs/2002AnGeo...20..953W/abstract>

The maximum of the smoothed sunspot number for cycle 22 was in July 1989; the minimum in May 1996, then heralded as the start of cycle 23, which peaked in April 2000. Each day of the years 1991 through 2000 is displayed in Fig. 1 as a traffic light presentation based on the 2-day fluences of >2 MeV electrons measured at geostationary GOES satellites. The days are ordered by 27.4-day Carrington solar rotations, starting with 1837 and ending with 1971; the righthand panel plots the smoothed sunspot number on a scale from 0 to 180. Black spots mark those days on which the mode switching anomalies occurred.

The outer belt electron enhancements (OBEEs) tend to last for several days but often exhibit a 27-day recurrence that reflects the persistence of coronal holes on the Sun. Their occurrence peaks not at solar maximum, but during the declining phase when high-speed streams of solar wind are more stable and long-lived. Although there is no direct correlation, the long-lived high-speed streams do occur during 1994 and 1995, approaching solar minimum, but not near solar maximum. A few bursts and associated OBEEs are obviously non-recurrent and appear to be associated with solar proton events, or perhaps coronal mass ejections. This solar cycle pattern fits well with earlier measurements made during cycle 21 (Baker et al., 1993).

Figure 3 reinforces the main message by showing the distribution of anomalies with respect to fluence, but it also explores the significance of season by plotting the switches against displacement from equinox (the line is a simple linear fit). Since coupling between the solar wind and the magnetosphere is easier near equinox, the electron fluences are generally higher and ESD [ElectroStatic Discharges] occurrence frequency can be expected to increase.

More info in these STCE Newsitems: <https://sidc.be/news/207/welcome.html> ,

<https://www.stce.be/news/463/welcome.html> , <https://www.stce.be/news/513/welcome.html> ,

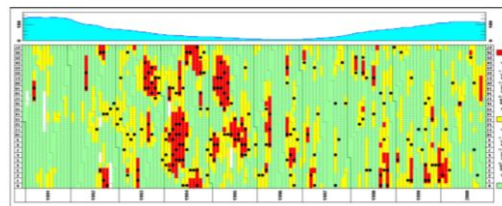
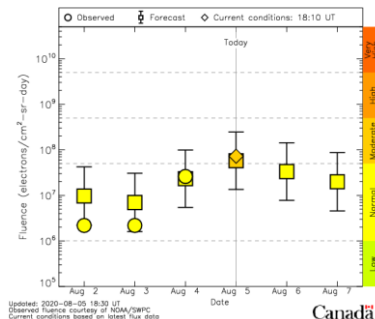
<https://www.stce.be/news/561/welcome.html>

Also at the STCE's SWx Classification page <https://www.stce.be/educational/classification#electrons> and

the STCE's SC25 Tracking page <https://www.stce.be/content/sc25-tracking#electron>

GNSS impacts from CH HSS

- High-Speed Stream (HSS)
 - Satellite charging
 - Deep di-electric charging
 - About 1 to few MeV e⁻
 - Deeply penetrate spacecraft (S/C)
 - Fluxes ≥ 2 MeV e⁻
 - Accumulation effect within S/C (ESD)
 - Due to day-night effect
 - Fluence (24h)
 - Declining phase solar cycle (coronal holes)
 - ~ 20 ESD/yr/GEO sat
 - Also strong ICME, e.g. 3-4 Nov 2021



39

An excellent discussion on how the high-energy electrons are generated is in High-speed solar-wind streams and geospace interactions

Kavanagh, Andrew; Denton, Michael in Astronomy & Geophysics, Volume 48, Issue 6, pp. 6.24-6.26, 2007
<https://ui.adsabs.harvard.edu/abs/2007A%26G....48f..24K/abstract>

As well as driving more obvious geomagnetic activity such as aurora, fast solar-wind streams also drive ultra-low-frequency (ULF) waves in the magnetosphere. These can transfer energy directly from the solar wind through the system to the ionosphere. These magnetic oscillations have periods ranging from 10s to 100s of seconds (known as Pc5 waves) and have been shown to depend strongly on solar-wind speed (e.g. Mathie and Mann 2000). The production mechanism for these waves is not completely understood, but a leading candidate is the Kelvin-Helmholtz instability at the magnetopause, which can energize waveguide modes that carry pulsation power into the inner magneto- sphere and ionosphere. Recent estimates based on observations suggest that the energy can be significant in comparison with substorms (e.g. Rae et al. 2007). One important aspect of the Pc5 waves is their potential ability to accelerate electrons to relativistic energy within the outer radiation belts (e.g. Elkington et al. 1999).

Relativistic electrons

One area that is the subject of a concentrated research effort is the mechanism for generation and loss of relativistic electrons in the radiation belts. Large geomagnetic storms can have drastic effects on the population of relativistic electrons in the inner magnetosphere; this can include the creation of new radiation belts at low latitudes (e.g. Baker et al. 2004). The effect of CIRs and HSSs on the relativistic electron flux is almost as dramatic. During CIRs dramatic drop-outs occur in the electron fluxes in the outer radiation belt; this is followed by a gradual increase to above pre-CIR levels during the HSS and subsequent decay. The cause of the initial drop-out is unknown, though there is evidence to suggest enhanced precipitation (e.g. Green et al. 2004) through possible interaction with a number of different magnetospheric waves. The mechanisms for accelerating electrons to MeV energies are clearly efficient. Radial diffusion through interaction with Pc5 waves is one possible mechanism and energy diffusion by cyclotron resonance with electromagnetic whistler mode waves is another. The relative strengths of these mechanisms are currently unknown but it is clear that acceleration is enhanced during HSSs (e.g. Mathie and Mann 2000).

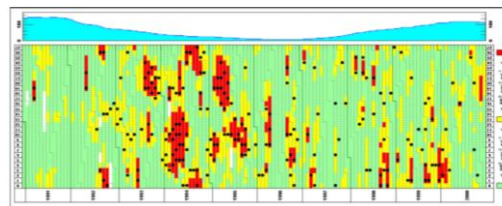
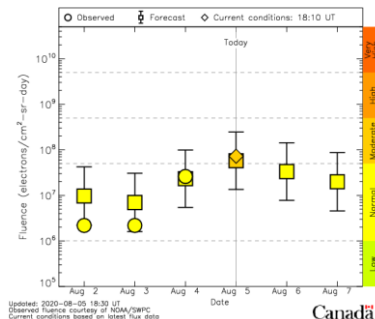
Also at Oulu: <http://magbase.rssi.ru/REFMAN/SPPHTEXT/ulf.html>

And Ham (2016): <https://agupubs.onlinelibrary.wiley.com/doi/pdf/10.1002/2016SW001492>

And Spaceweather.com: <https://www.spaceweather.com/archive.php?view=1&day=10&month=03&year=2020>

GNSS impacts from CH HSS

- High-Speed Stream (HSS)
 - Satellite charging
 - Deep di-electric charging
 - About 1 to few MeV e⁻
 - Deeply penetrate spacecraft (S/C)
 - Fluxes ≥ 2 MeV e⁻
 - Accumulation effect within S/C (ESD)
 - Due to day-night effect
 - Fluence (24h)
 - Declining phase solar cycle (coronal holes)
 - ~ 20 ESD/yr/GEO sat
 - Also strong ICME, e.g. 3-4 Nov 2021



40

Alerts:

SWPC: <https://www.swpc.noaa.gov/products/goes-electron-flux>

The electron flux measured by the GOES satellites indicates the intensity of the outer electron radiation belt at geostationary orbit. Measurements are made in two integral flux channels, one channel measuring all electrons with energies greater than 0.8 million electron Volts (MeV) and one channel measuring all electrons with energies greater than 2 MeV.

Electron Event ALERTS are issued when the >2 MeV electron flux exceeds 1000 particles/(cm² s sr). High fluxes of energetic electrons are associated with a type of spacecraft charging referred to as deep-dielectric charging. Deep-dielectric charging occurs when energetic electrons penetrate into spacecraft components and result in a buildup of charge within the material. When the accumulated charge becomes sufficiently high, a discharge or arcing can occur. This discharge can cause anomalous behavior in spacecraft systems and can result in temporary or permanent loss of functionality.

Forecast at <https://www.swpc.noaa.gov/products/relativistic-electron-forecast-model>

NRCan: <https://www.spaceweather.gc.ca/forecast-prevision/space-spatiale/sffl-en.php>

SWS: <http://www.sws.bom.gov.au/Satellite/3/1>

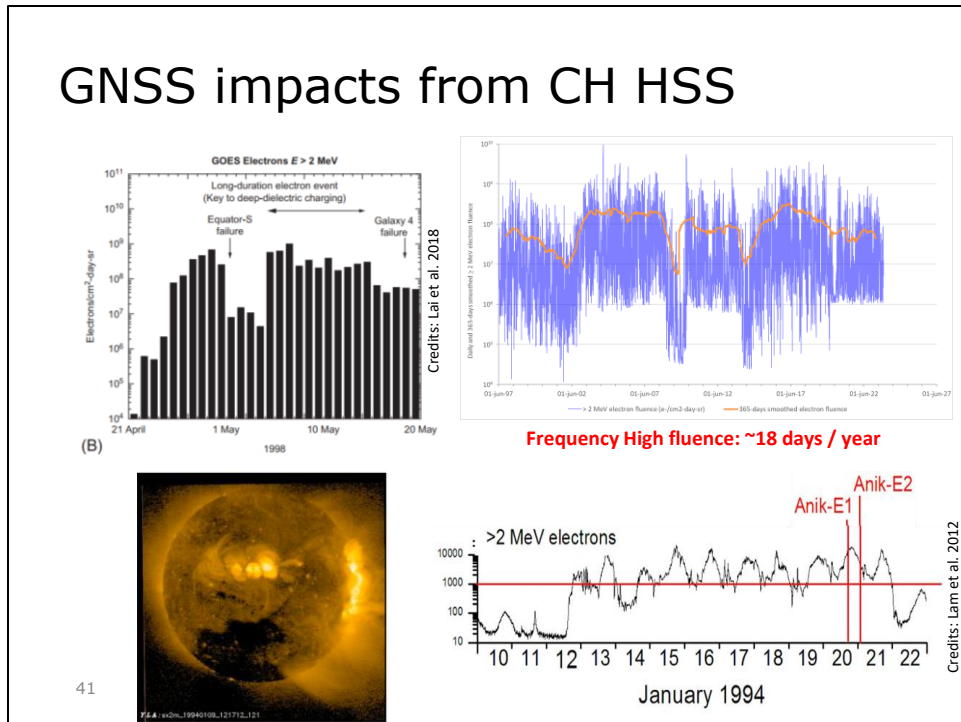
SIDC: <https://www.sidc.be/>

Also at Baker et al. (2004): Characterizing the Earth's outer Van Allen zone using a radiation belt content index <https://ui.adsabs.harvard.edu/abs/2004SpWea...2.2003B/abstract>

Figure 7b shows the RBC index plotted as a 27-day running average from 1992 to 2001 (upper curve). Plotted below this is the 27-day running average of the solar wind speed, VSW. *It is striking that the running-averaged values of VSW were significantly greater than 500 km/s only in 1994. That obviously was the time of the highest radiation belt electron content as well.*

Another good website on deep di-electric charging is from the Australian Space Academy: <http://www.spaceacademy.net.au/spacelab/models/ddd.htm>

GNSS impacts from CH HSS



Upper right figure is from the STCE's SC25 Tracking webpage <https://www.stce.be/content/sc25-tracking>
 More info also at <https://www.stce.be/educational/classification#electrons>
 The highest electron fluence since 1997 was recorded on 29 July 2004, when it reached a value of $9.3 \cdot 10^9$ electrons / (cm² sr day). From 2003 to 2008, and again from 2015-2019, elevated fluence levels were recorded because of the declining phase of the solar cycle when (equatorial) coronal holes and the extensions of polar coronal holes are most numerous. The two dips early 2002 and mid 2014 mark solar cycle maximum when the polar magnetic fields were reversing their polarity and coronal holes were pretty much absent and in the process of being recreated.

A period of enhanced (moderate to high) levels of electron fluence was recorded from 5 till 14 September 2022. Operators reported numerous satellite glitches at the end of the period, in particular a few days after maximum fluence on 8 September. This shows again the importance of the electron accumulation effect on the satellite's instruments.

From 2 June 1997 till 5 February 2023, there have been 471 days with high fluence ($> 5 \cdot 10^8$ electrons/cm² sr day). This is an average of about 18 per year.

Figure at the upper left:

Fig. 7 from Lai et al. (2018): Deep Dielectric Charging and Spacecraft Anomalies

DOI: 10.1016/B978-0-12-812700-1.00016-9

https://www.researchgate.net/publication/323630151_Deep_Dielectric_Charging_and_Spacecraft_Anomalies

Original figure 3a from Baker et al. (1998) - Disturbed Space Environment May Have Been Related to Pager Satellite Failure

<https://doi.org/10.1029/98EO00359>

Two other figures from Lam et al. (2012): Anik-E1 and E2 satellite failures of January 1994 revisited

<https://agupubs.onlinelibrary.wiley.com/doi/full/10.1029/2012SW000811> (Fig. 1a and 3)

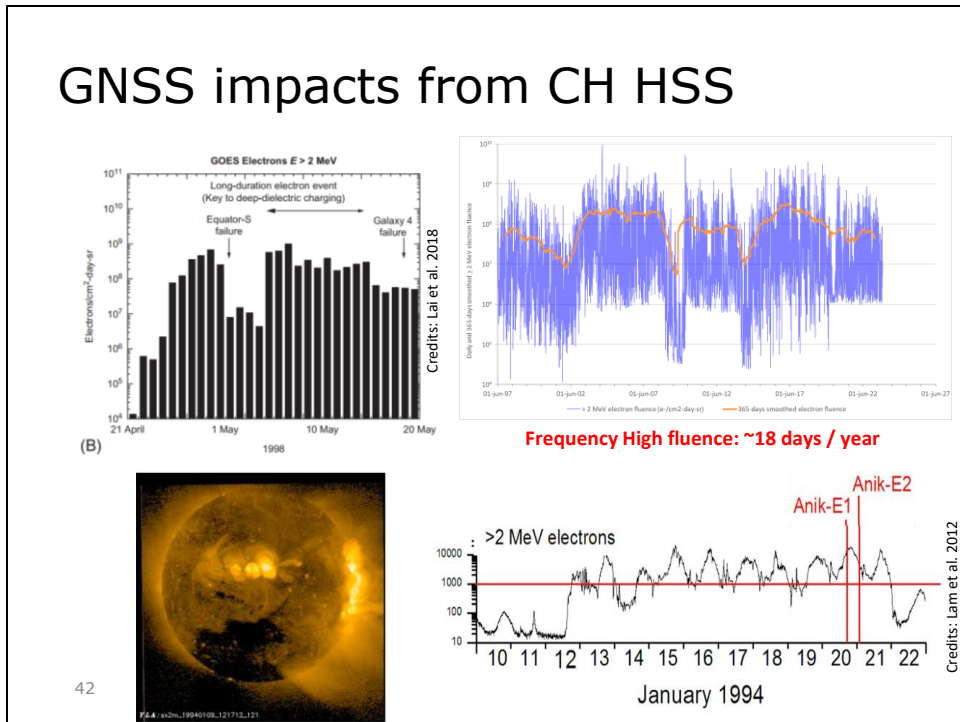
Failure of the ANIK-1 and -2 satellites occurred during a substorm following active to minor storming activity from a number of CHs (13-19 January). Both satellites were recovered, but at a cost of about \$50-70 million, and plenty of problems for cable TV, telephone, newswire and data transfer services throughout Canada.

<http://www.solarstorms.org/SWChapter6.html>

Leach and Alexander (1995): Failures and anomalies attributed to spacecraft charging

<https://ntrs.nasa.gov/search.jsp?R=19960001539>

GNSS impacts from CH HSS



Upper right figure is from the STCE's SC25 Tracking webpage <https://www.stce.be/content/sc25-tracking>
 More info also at <https://www.stce.be/educational/classification#electrons>
 The highest electron fluence since 1997 was recorded on 29 July 2004, when it reached a value of $9.3 \cdot 10^9$ electrons / (cm² sr day). From 2003 to 2008, and again from 2015-2019, elevated fluence levels were recorded because of the declining phase of the solar cycle when (equatorial) coronal holes and the extensions of polar coronal holes are most numerous. The two dips early 2002 and mid 2014 mark solar cycle maximum when the polar magnetic fields were reversing their polarity and coronal holes were pretty much absent and in the process of being recreated.

A period of enhanced (moderate to high) levels of electron fluence was recorded from 5 till 14 September 2022. Operators reported numerous satellite glitches at the end of the period, in particular a few days after maximum fluence on 8 September. This shows again the importance of the electron accumulation effect on the satellite's instruments.

From 2 June 1997 till 5 February 2023, there have been 471 days with high fluence ($> 5 \cdot 10^8$ electrons/cm² sr day). This is an average of about 18 per year.

The highest value since 1997 occurred on 29 July 2004 when the daily electron fluence reached a value of $9.3 \cdot 10^9$ e- / cm² sr day. The electron flux peaked near $\sim 300,000$ pfu following the passage of a trio of strong fast ICMEs in the previous days.

Meredith et al. 2016 - Extreme energetic electron fluxes in low Earth orbit: Analysis of POES E > 30, E > 100, and E > 300 keV electrons
<https://agupubs.onlinelibrary.wiley.com/doi/10.1002/2015SW001348>

Two of the top five largest fluxes of E > 300 keV electrons at L* = 6.0 occurred in late July 2004. These events occurred during the three strong storms that eventually lead to the largest flux of E > 2 MeV electrons observed at GOES over the 20 year period from 1995 to 2014 [Meredith et al., 2015]. During this event Galaxy 10R lost its secondary ion propulsion system, used to maintain its in-orbit position, reducing its lifetime significantly [Choi et al., 2011] and resulting in an insurance payout of U.S. \$75.3 million (Seradata SpaceTrak Launch and Satellite Database, www.seradata.com).

The 3 strong geomagnetic storms can be seen in the Dst evolution at WDC Kyoto: https://wdc.kugi.kyoto-u.ac.jp/dst_final/200407/index.html

Summary

- GNSS applications impacted by extreme SWx:
 - Solar flares
 - Solar radio bursts
 - Geomagnetic storms (ICMEs)
 - Ionospheric storms
 - Ionospheric scintillations
- GNSS satellite fleet may suffer from:
 - Charging effects
 - Solar energetic particle events
 - Deep di-electric charging
 - ...

